UNIVERSITY OF TWENTE.

Fabrication of solid polymer layer of poly-methyl methacrylate mixed with Lumogen F Red 305 for the use in Free Space Luminescent Solar Concentrators.

Vijayakumar Akshay Kumar

Master Thesis

Inorganic Material Science

Masters Sustainable Energy Technology, University of Twente

July, 2022

Supervisor:

Dr. R. Saive

Graduation Committee:

Prof. Dr. Ir. J.E. Ten Elshof

Dr.Dipl.-Ing. E. Shirazi

Dr. R. Saive

Abstract

In countries with predominant overcast weather like the Netherlands, the portion of direct sunlight received is 45%, and the rest is diffused light. Conventional solar concentrators cannot concentrate diffused light due to thermodynamic reasons. One of the methods to overcome this barrier are luminescent solar concentrators (LSCs), which can concentrate direct and diffused sunlight and re-emit them on a solar panel. This process further increases the yield of a solar panel on a cloudy day, making this technology a viable solution for higher solar energy production.

One of the methods to overcome this barrier on an overcast day is by incorporating technologies such as luminescent solar concentrators (LSCs). LSCs collect diffuse light over a large area, convert it into luminescence, and then concentrate this longer wavelength of collimated light onto a solar cell. However, efficiencies of conventional LSCs have been limited due to loss mechanisms associated with multiple processes such as the luminophore quantum yield, reabsorption/emission rates, parasitic waveguide absorption and unwanted escape. LSCs trap the converted luminescent light in the waveguide, which is then redirected to a solar panel attached to the edge of the waveguide. Free-space luminescent solar concentrators (FSLSCs) present a paradigm shift to reduce these loss mechanisms and allow the converted luminescent light to escape under a narrow escape cone. This remitted, concentrated light is then directed to a solar panel, placed at a distance from the concentrator. FSLSCs consist of a nanophotonic coating, a luminophore-embedded polymer film coated on the sides and the back of the film with a white paint acting as a Lambertian back reflector. FSLSCs provide a shorter optical path length for the converted luminescent light to travel when compared with the LSCs and increases the power per solid angle of the re-emitted light, which is redirected onto solar panels.

This research primarily focuses on developing the polymer waveguide containing the luminophores and optimising the experimental parameters for the fabrication process used in the FSLSC. The medium used to embed the lumogen red dye is poly methyl methacrylate (PMMA), which has excellent light transmission properties of 92% transmittance with a thickness of 3 millimetres. Therefore, the lumogen red dye is dissolved in PMMA by a solution and cast into moulds. This experiment is carried out for different concentrations of PMMA and the lumogen red dye. Photoluminescence of each Lumogen embedded waveguide is characterised by its optical properties to ensure maximum quantum efficiency. Finally, a waveguide with

the highest photoluminescent quantum efficiency of 98% is used to test the overall performance of the FSLSC.

Contents

Chapter 1

Introduction

To ensure that the effects of climate change are reduced, a transition needs to be made from fossil fuels to a more sustainable method. This transition can be achieved with many different technologies but solar power is one of the major contributors. By the use of photovoltaic's (PV), electricity generation is expected to provide 15% of the global energy consumption [1]. This would mean a drastic increase in the total quantity of installed solar panels, as well as an reduction in the cost of power generated by the panels. A method to lower the cost of solar power is by increasing the output of each individual panel. This can be achieved by increasing their conversion efficiency, or by concentrating sunlight from larger areas onto smaller areas of a solar panel.

A solar panel or module typically consists of multiple solar cells put together. Each solar cell contains a semiconductor junction that absorb light energy above its bandgap. The absorption of light creates an electron-hole pair inside the junction. Now, splitting this pair of electron-hole generates a current that can be collected at the contacts. The voltage caused by the generated current is closely related to the bandgap of the material which is absorbing light.

The theoretical maximum efficiency is limited by the Shockley–Queisser limit. For a single junction silicon cell, the Shockley–Queisser limit is 32% [2]. Efficiencies of 26.6% can be seen experimentally by mono-crystalline silicon cells, which is at 83% of the theoretical limit [3]. It can be concluded that the efficiency of a silicon solar panel is almost at its maximum limit.

One method to over the barrier of the Shockley–Queisser limit is to focus sunlight on a spot to generate heat, and then convert this heat energy to electrical power using heat engines. This methodology does incorporate the use of semiconductor junctions and do not have to follow the Shockley–Queisser limit. With parabolic dish concentrators, they work on focusing the light on a stirling engine and generator to convert the heat to electricity. A conversion efficiency of 25% to 30% can be achieved with this methods [4]. One disadvantage of this technology is that a

tracking system needs to be installed, so that the concentrator can track the sun all throughout the day to achieve optimal focusing.

In a research published in 2017, it was found that the Netherlands receives 45% of direct incident sunlight and the rest of the light is diffuse light [5]. Diffuse light lowers the potential of the concentrating solar power systems, since diffused light cannot be focused using mirrors or lenses. [6]. The conversion efficiency of a solar cell is reduced when it is subjected to diffuse light when compared to direct sunlight of AM 1.5. When light is normally incident light on a solar panel its efficiency is the highest [7] [8]. A method to over come this barrier is by using a technology called luminescent solar concentrator (LSC). LSC are able to capture this diffuse light and are able to increase the output of a solar panel on a cloudy day. [9].

Chapter 2

Background Information

This section describes the background information required for the research to be carried out. The first section of this chapter 2.1 mentions about luminescent solar concentrators and its working principle. The following section 2.2 describes a method to further increase the power output of a solar panel in diffuse conditions by using the Free-Space Luminescent Solar concentrator (FSLSC). In this part of the chapter, the section explains the concept of the components associated with the Free-Space Luminescent Solar Concentrator and its working principles.

2.1 Luminescent Solar Concentrators

A method to concentrate diffuse light is by using the Luminescent Solar concentrator (LSC) technology. This method was first proposed in 1970's [10]. A luminescent solar concentrator consists of three things, the first component being a transparent polymer layer, the second component being a dye molecule with luminescent properties which is infused in the polymer layer. The luminescent particles present in the polymer layer is capable of absorbing diffuse light consisting of lower wavelengths and direct sunlight. They then emitting a light at a higher wavelength. This emitted light is trapped inside the polymer and travels to the edges of the polymer. The third component is a small high efficiency solar cell that is placed at the sides of the polymer to receive the emitted light. [11].

2.1.1 Working of LSC

LSC have a property to capture diffuse light that is incident on the surface of the polymer layer mixed with luminophores. Diffuse light consist of different wavelengths of light from the solar spectrum and as they are incident on the top of the polymer layer mixed with the luminophore, they strike the luminophore present in layer and emit light of higher wavelength. This emitted light is guided by the polymer layer which acts as a waveguide to concentrate the light at the sides of the

polymer layer. LSC works as a diffuse light concentrator by collecting all the light from the top, guiding them and concentrating them at the sides of the layer. The waveguide is not a very thick polymer layer, making the size of the solar panels attached to it quite small [12]. The working of the LSC can be depicted by the figure 2.1. Highest recorded conversion efficiency of a LSC which has been recorded by far is 7.1% [13].

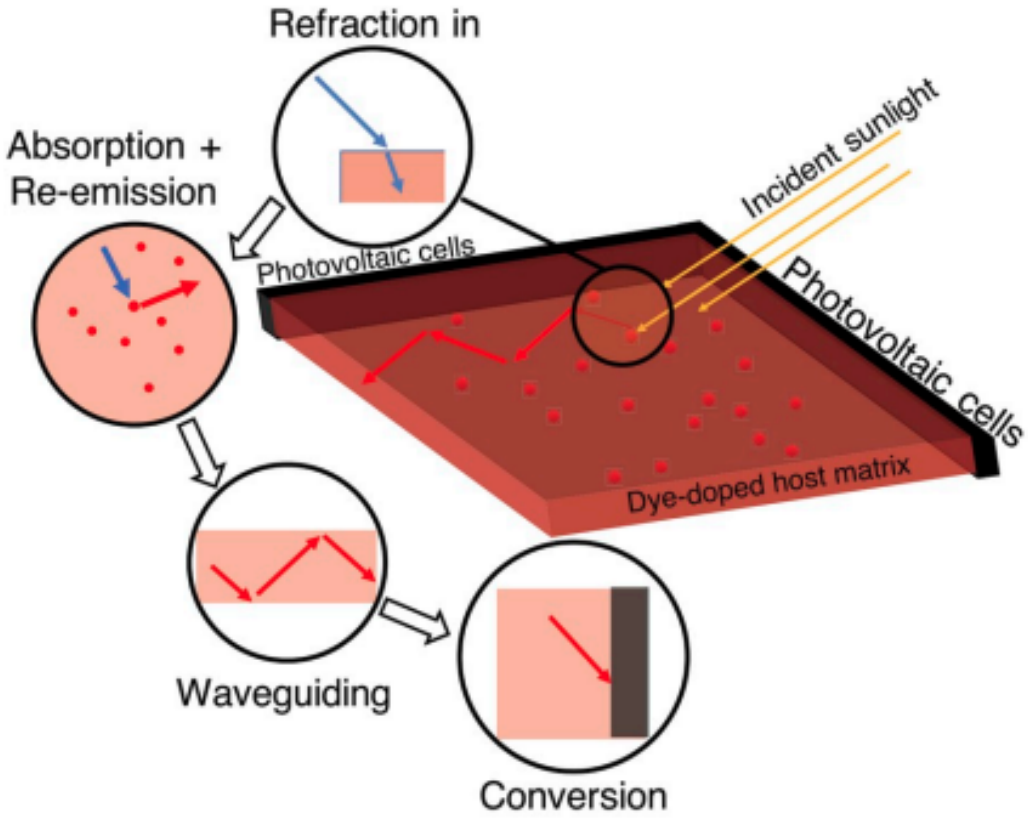

FIGURE 2.1: The following figure shows the working of an LSC device, referenced from: [14]

2.1.2 Merits and demerits of LSC Technology

LSC have quite a few merits for its applications. To begin with, the waveguide materials used in an LSC are inexpensive for fabrication when compared to a solar panel of similar dimensions [11]. They also offer a potentially lower cost per Wp produced [15]. Majority of the LSC use fluorescent organic dyes, due to a broad absorption spectra and high conversion efficiencies of light. Research has further led to using quantum dots [16][17], or nano-crystals [18]. By using these materials the emission spectra of the luminophore can be finetuned precisely. But since such

devices suffer from large reabsorption due to overlap of the emission and absorption spectra, or low quantum efficiency of the luminophores in the layer.

Another point to be noted is that although the highest conversion efficiency is 7.1%, it is not high enough for the use of LSC to be implemented on a wide scale for power conversion [18]. Extensive research has been conducted for finding other implementations of the LSC. Since LSC are not meant for high power conversions, it can be used for power generation in areas where it is not possible to generate electricity with a solar panel. Semi-transparent LSC moduels can be integrated in windows [19] [20] or on the side of buildings [21]. But the majority of the losses associated with the LSC is due to reabsorption of emitted light within the waveguide. This is due to the large path length the emitted light has to travel to reach the solar panel.

2.2 FSLSC

In LSC the emitted light needs to travel a long path-length during which majority of the absorption losses occur. The light incident on the surface of the LSC is absorbed and light is emitted which has to travel a long way through a dense medium before it reaches the solar cell placed at the edge. A method to overcome this barrier is to not trap light inside the dense polymer medium, but instead to let it escape out into air through a narrow escape cone [22]. A technology to implement this theory is the Free-Space Luminescent Solar Concentrator (FSLSC) [22]. In this technology the collimated light travels through free-space rather than a dense polymer medium. The output of the FSLSC is not high intensity light in a smaller area, instead it is collimated light which can be redirected towards external solar panels place at a distance. Instead of increasing the intensity of diffused incoming light like a conventional LSC, the FSLSC increases the power per solid angle [23].

2.2.1 FSLSC's components

The next three subsections describe the individual components which the FSLSC module consists of. The FSLSC module has three main components. 1. A nanophotonic coating 2.3, 2. A polymer layer embedded with lumogen dye 2.2.1, and 3. A diffuse back reflector 2.2.1.

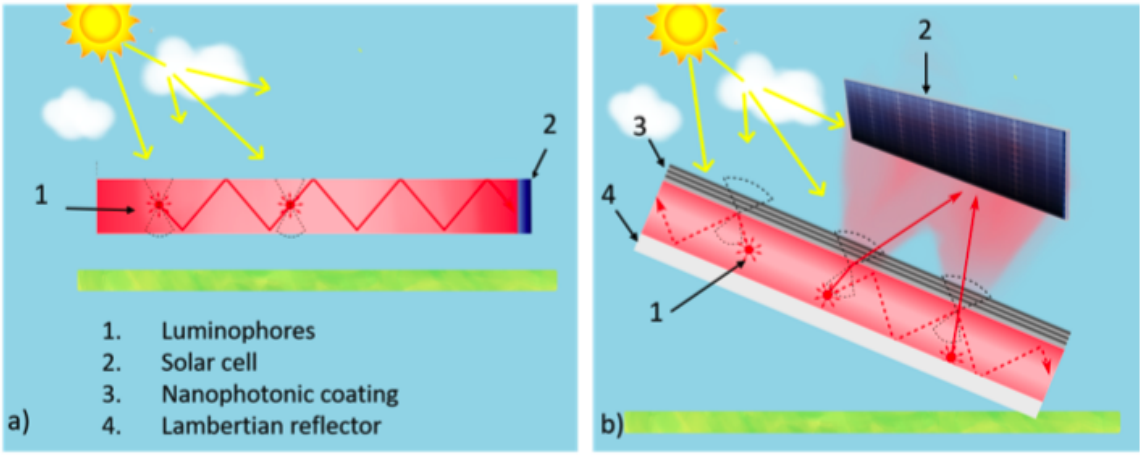

FIGURE 2.2: (a)Conventional LSC (b) FSLSC. LSC uses wave-guiding to transfer the emitted light to a solar panel at the edge of the device, while FSLSC allows light to escape in a narrow escape cone that can be directed towards external solar panels, referenced from [24].

Nanophotonic coating

The top surface used in the FSLSC requires special reflectance properties. This can be accomplished by using a nano-photonic coating which consists of layered structures of alternating materials that comprise of different refractive indices. Such a structure with many layers induces multiple interfaces where light is reflected. Partially reflected individual light waves interfere with each-other to generating a combined reflected wave. This interference of light is schematically shown in figure 2.3. It is possible to calculate the reflectance of such a stack analytically given the layer thicknesses and refractive indices.

Polymer layer housing Lumogen F RED 305

The polymer layers used in LSC applications are also used as the waveguide in the FSLSC. The polymer used in the wave-guide is polymethyl methacrylate (PMMA). The dye that is used in the polymer layer is the lumogen f red 305. This research's main focus is to fabricate the polymer layers mixed with the luminophore dye and then characterize it.

Polymethyl methacrylate polymer layer: Polymethyl methacrylate is a synthetic resin which is produced from the polymerization of methyl methacrylate [25]. It is a transparent rigid plastic that is used as a substitute for glass in products such as shatter proof windows and skylights. Its trademark names are Plexiglas, Lucite, and Perspex. PMMA is known for its optical properties to transmit light. The PMMA polymer used in this research has a density of 1.18 g/cm^3 and with light

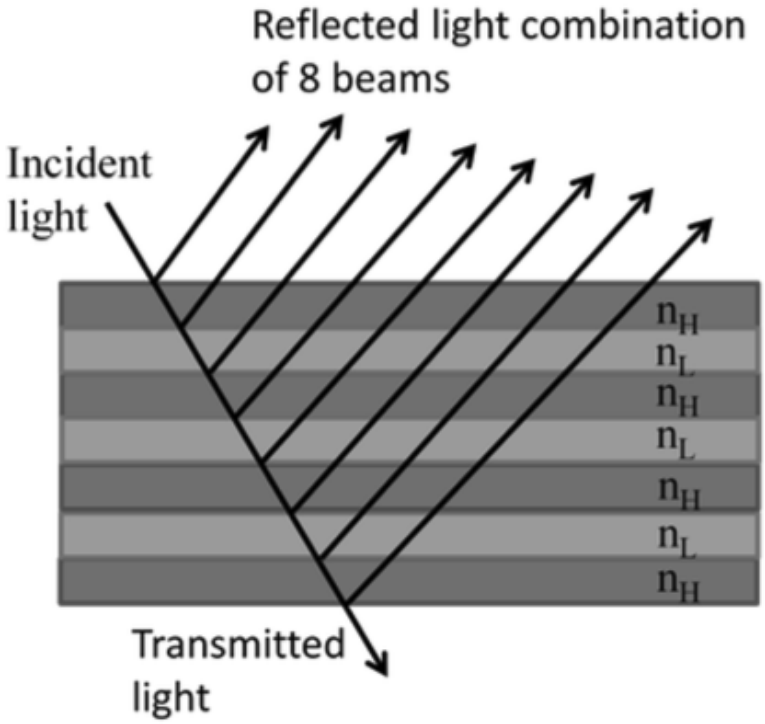

FIGURE 2.3: The image shows partial reflections on each interface in a dielectric stack, interfere with each-other to create total reflectance, referenced from [24].

transmittance of 92% with thicknesses of upto 3mm [26]. PMMA is soluble in variety of organic solvents such as toluene, benzene, xylene etc. [27]. The following figure 2.4 depicts the monomer structure in PMMA that acts as the repeating units. In this research PMMA acts as the polymer medium to house the lumogen red dye.

Lumogen F Red 305: The luminophore used in this research is the Lumogen F red 305 dye manufactured by BASF. The lumogen red dye is a very common and popular dye used in the LSC research due to its high quantum yield and its broad range of absorption spectrum [29]. The reported quantum yield for the lumogen red dye ranges between 95% to 100% [30] [31].The Lumogen red dye is a dark red powder with a density of 450 kg/m^3. Its molecular structure is shown in figure 2.5. The lumogen red dye dissolved in toluene will be used in the development of the polymer layer for the FSLSC.

Diffuse back reflector

Diffuse reflectors are also called Lambertian reflectors as they are defined by Lambert's cosine law of reflection. A Lambertian surface randomizes incident light, such

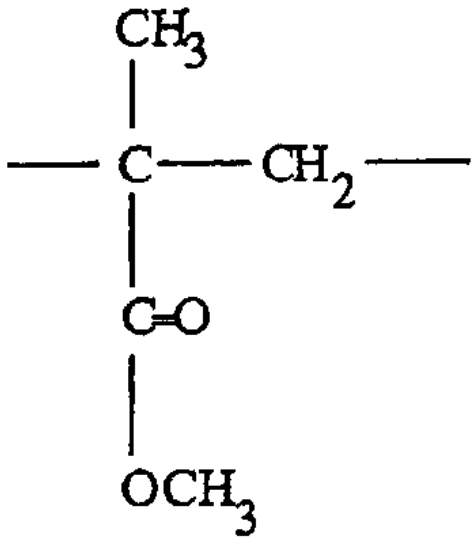

FIGURE 2.4: Figure shows the monomer structure in PMMA that acts as the repeating units, referenced from: [28].

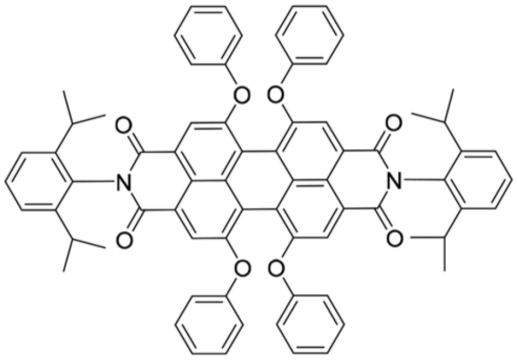

FIGURE 2.5: Figure shows the molecular structure of the Lumogen F RED 305 Dye, referenced from: [32].

that the intensity of the reflected light is proportional to the cosine of it's angle with respect to the surface's normal. This is depicted in figure 2.6. The reflection of a Lambertian reflector is independent of the incoming angle of light. This property allows it to perfectly randomize the direction of incoming light.

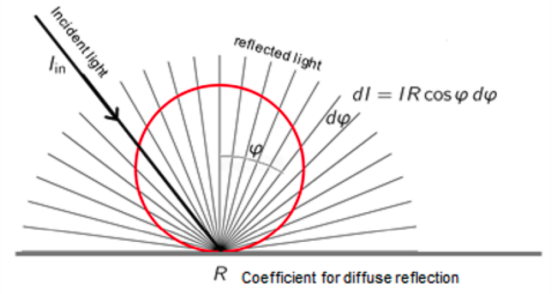

FIGURE 2.6: Figure shows the reflectance of a diffused surface. The red circle denotes angle-dependent intensity of diffuse reflections, referenced from: [24].

2.2.2 Working of FSLSC

The FSLSC module mainly consists of three components. A nano-photonic coating, a polymer layer embedded with lumogen dye, and diffuse back reflector. These components can be depicted by figure 2.7. Diffuse light, which is incident at all angles on the nano-photonic coating, passes though an entry cone. This light is directed onto a polymer layer, which is embedded with luminophore dye. The luminophores present in the polymer layer enables light of lower wavelength to be converted to light of higher wavelength. The emitted light is trapped inside the waveguide. The use of the Lambertain back reflector randomises the emitted light and reflects it upward. If the ray reaches the nano-photonic coating, it leaves the system, else the emitted light is reflected back down. When the emitted light reaches the bottom, the cycle repeats until each ray has left the system. As red shifted emitted light reaches the nano-photonic coating, due to its inherent properties the red-shifted light is only transmitted in a narrow cone. Meaning that the red-shifted light that leaves the FSLSC is collimated.

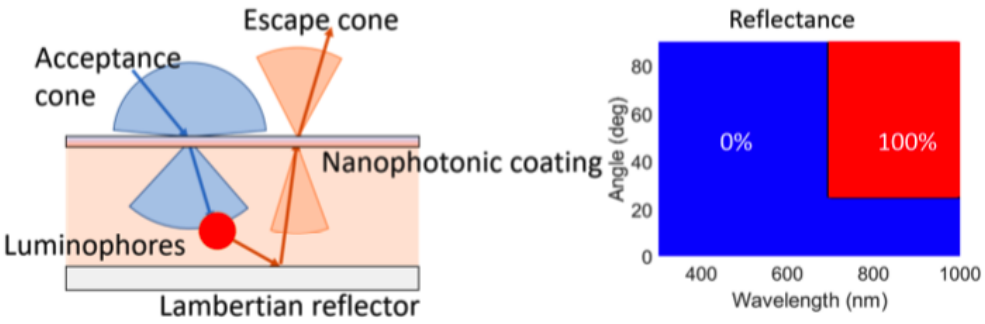

FIGURE 2.7: Left, FSLSC working principle with its components. Right, reflectance of the nanophotonic coating which transmits all incident blue light, but only allows red light to leave within a narrow escape cone, referenced from: [24].

Chapter 3

Experimental Techniques

This chapter describes the step-by-step methods involved in the experimental techniques used to the fabricated the polymer layer mixed with the Lumogen f red 305. The First section (3.1) explains the the preparation of the lumogen f red 305 dye solution. Then section (3.2) explains the preparation of the polymer solution. Then the two solutions i.e. the lumogen red 305 dye solution and the polymer solution are mixed thoroughly. The next section (3.3) describes the fabrication of the polymer layers. The following section (3.4) describes the application of the Lambertian reflector on the fabricated layers. Finally the section (3.5) describes the method for the FSLSC prototype assembly.

3.1 Preparation of Lumogen F Red 305 Dye Solution

To utilize the Lumogen Red 305 dye, it has to be dissolved in a solvent. This procedure is carried out by dissolving the dye in toluene. As toluene is the best known common solvent to dissolve the dye, as its optical properties are ideal [32][33]. The experiments are performed in the chemical laboratory. When using the lumogen red dye in LSC applications, they usually range between 10ppm - 100ppm. This is due to the fact that area for the the optical cross-section which is required, is very low [30] [32]. The lumogen red dye is a very light solid particle of 450 kg/m^3[33]. Which means that very little quantity of it is required. First a stock solution is made with toluene and the dye. 34.5 mg of dye is weighed out on a calibrated weighting scale and 25ml of toluene is titrated into the container containing the dye with a pipette. The mass concentration of around 1600 ppm, and is too high of a concentration for the intended purpose. This means that the dye needs to be further diluted.

The first step would be to make liquid samples and then solid samples. Small quantities of the stock solution are mixed with toluene to create the liquids samples housing the lumogen dye. Five different concentrations are studied with the Lumogen F Red 305. These concentrations are obtained by diluting the dye solution with toluene in a magnitude of 6-10 times to obtain the final solutions. The dilutions can

be performed with the aid of bulb volumetric pipettes. The concentrations used in the liquid sample measurements are shown by the table 3.1. Appendix 8.34 gives the calculations involved in estimating the concentration of the lumogen dye solutions.

No.	Stock(mL)	Toluene (ml)	Concentration (PPM)
1	0.15	6	38.70
2	0.30	6	75.56
3	0.50	6	122.07
4	0.75	6	176.34
5	1.0	6	226.73

TABLE 3.1: Tables gives the list of concentrations used for the Liquid samples

3.2 Preparation of housing solution, PMMA in Toluene

The next step involved is to create the solid housing medium for the lumogen red dye. This process involves converting PMMA that is present in the form of granules to a solution. Toluene is a good solvent to completely dissolve PMMA at normal room temperature and pressure [34]. Due to PMMA being miscible in toluene and also the dye being miscible in toluene, these two solutions can be mixed further to create the solutions required for the fabrication of the polymer layers mixed with lumogen red dye.

For this study, varying concentrations of PMMA are mixed with toluene to produce various solutions of PMMA in toluene. This method is done by weight % of PMMA in toluene. Concentrations of 3.3%, 10%, 15%, 20% & 30% of PMMA in toluene by weight is made in the lab and mixed thoroughly. Now the PMMA in toluene solution are ready and can be mixed with the standard stock dye solutions. This mixing is done in the same ratio as the previous section with the liquids, i.e. 6ml of 3.3% PMMA in toluene (by weight) is mixed with 0.15 ml, 0.30ml, 0.50ml, 0.75ml, 1.0ml of the stock lumogen dye solution. The concentrations of these solutions can be given by the table 3.2.

3.3 Fabrication of polymer layer mixed with Lumogen F Red 305

The next step involved is the fabrication of the polymer layers. This section describes how solid polymer layers mixed with lumogen red are fabricated. The mixed solution of PMMA and lumogen dye in toluene are cast into a petri dish, the volatile

No.	Stock(mL)	3.3% (by weight%) PMMA in Toluene (ml)	Concentration (PPM)
1	0.15	6	38.1
2	0.30	6	74.16
3	0.50	6	119.33
4	0.75	6	171.56
5	1.0	6	219.64

TABLE 3.2: Above is the list of concentrations used with stock solution of dye dissolved in PMMA

content present in the solution (i.e. toluene) evaporates leaving behind a solid polymer layer mixed with the lumogen red dye. The petri dish acts as a mould for the polymer layer mixed with the dye to take its shape. The petri dishe is a borosilicate glass and by its nature is a hydrophilic layer [35]. This means the solid polymer layer cast onto the petri dish will bind to it.

To avoid this phenomenon the petri dish is silanized to make it hydrophobic in nature [36]. This process is preformed in two steps where in the first step would be to remove all the organic residue on the surface by oxidizing the petri dish in the plasma chamber. Once that is accomplished, silanization can be performed in a closed box. In this step, grease is added to the surface of the petri dish that is in contact with the desiccator. The silanizing agent is added to the petri dish surface and the desiccator is closed and the sample is left over night.

After the petri dishes are silanized, they can be used for fabricating the polymer layers with the lumogen dye. The method used for fabricating the polymer layer with the dye, is separation of volatile compounds from polymer by drying. The concentrations mentioned in table 3.2 are cast into the petri dishes using volumetric pipettes and are left to dry over night. Five layers of increasing concentrations are obtained with 3.3% PMMA (weight %) with concentrations of 38.1 PPM, 74.16 PPM, 119.33 PPM, 171.56 PPM, 219.64 PPM.
An observation can be made that the layers that are fabricated are too thin and the thickness of the samples should be increased. The first method chosen to increase the thickness of the polymer layer, is to increase the weight% of PMMA in the solution of PMMA in toluene. The concentrations of PMMA in toluene used is 10%, 15%, 20% & 30% by weight%. To each mentioned weight concentration the different quantities of the stock solution are added and fabricated. With increasing weight% of PMMA in toluene, the desired result of thickness of around 3mm is achieved. But with increasing PMMA concentration has made the solutions more viscous, leading to formation of bubbles within the polymer layer after drying.

To overcome this phenomenon the concentration of PMMA in toluene is reduced back to 3.3% PMMA in toluene (weight%), and multiple layers are cast one on top

of the other after each preceding layer is dried. This is done for one to six layers of 3.3% PMMA in toluene (weight%) with concentrations of 38.1 PPM, 74.16 PPM, 119.33 PPM, 171.56 PPM and 219.64 PPM.

The next step in the process is to perform the measurement techniques on these samples to check for absorption and photoluminescence quantum efficiency.

3.4 Application of spectralon to polymer layers

After the measurement techniques on the fabricated samples are performed, the next step is to select the ideal polymer layer with the highest photoluminescence quantum efficiency. This layer will be used in the construction of the FSLSC. But for it to be used in the FSLSC module, the polymer layer must be coated with a highly diffuse reflective material called Spectralon. First the polymer layers are cleaned with ethanol and then Spectralon paint is applied. Since the Spectralon material is highly viscous, it is diluted with a mixture of water and ethanol to the desired quantity. This coating is then painted on the polymer layer, in such a way that all the sides except one face of the polymer layer are coated. The polymer layer is coated in such a manner that there is at least two to three millimeter thickness of Spectralon on the polymer layer. This is depicted in figure 3.1, 3.2.

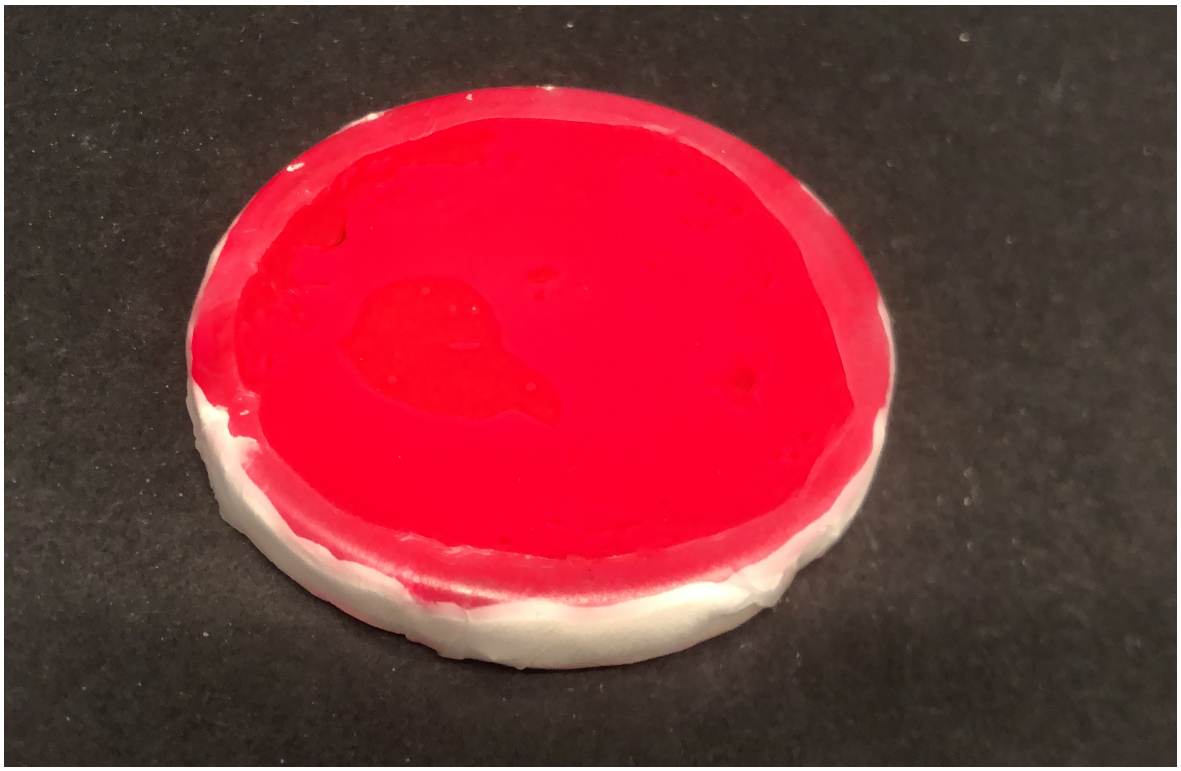

FIGURE 3.1: Top part of polymer layer with dye coated with Spectralon

FIGURE 3.2: Bottom part of polymer layer with dye coated with Spectralon

3.5 Assembly of prototype

The final FSLSC module consists of the polymer layer mixed with dye that is coated by a Lambertian reflector on all sides, except the top. On the top of the polymer layer, mixed with the dye, there is a layer of water which is put in between the nano-photonic coating and the polymer layer. The usage of water in this system is very important. It helps to remove the air interface between the polymer layer and the nano-photonic coating. Without the use of water, the light inside the concentrator will undergo total internal reflection. This is shown in figures 3.3, 3.4.

The image on top shows how light undergoes total internal reflection due to the air gap. The bottom image shows how water negates the effect of total internal reflection. Water is used as an index matching layer. Air has a lower refractive index when compared to the nano-photonic coating. Whereas, water has a similar refractive index as the nano-photonic coating reducing the total internal reflection.

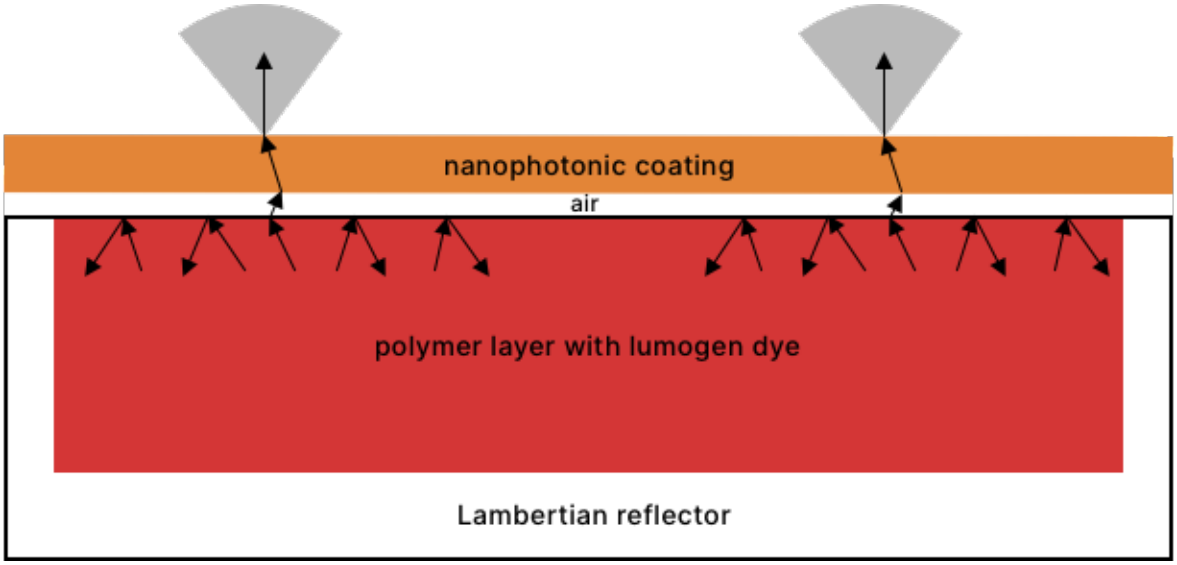

FIGURE 3.3: Effect of total internal reflection due to air gap

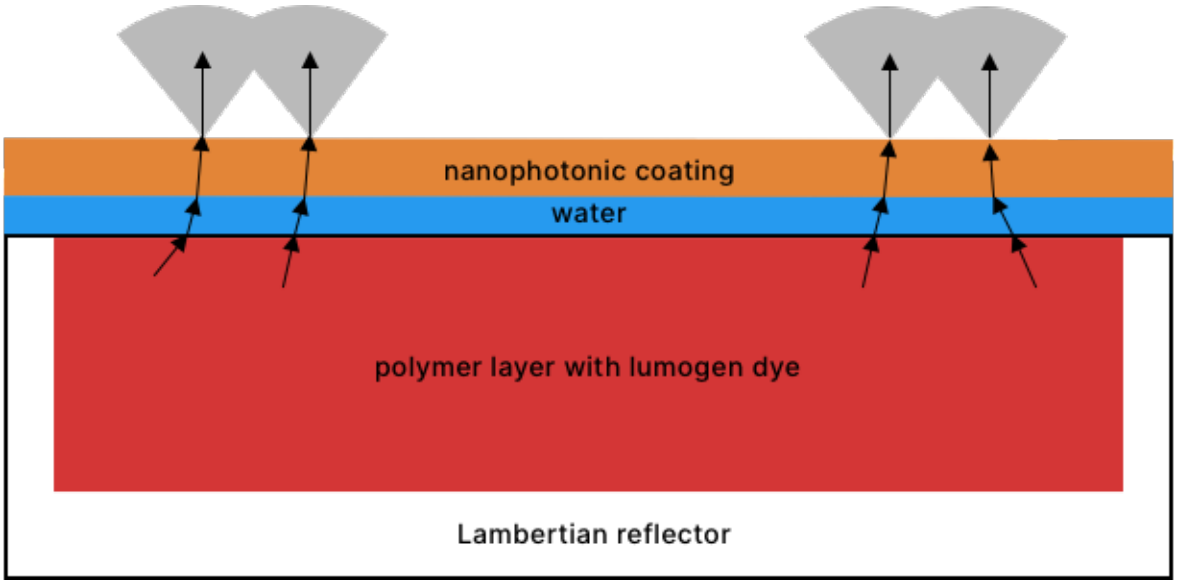

FIGURE 3.4: Image shows how water negates the effect of total internal reflection of light

Chapter 4

Measurement Techniques

This chapter describes the measurement techniques used to measure the optical properties of the fabricated polymer layer mixed with the Lumogen f red 305. The First section (4.1) explains the working of the Perkin Elmer Lambda 950 Spectrophotometer that is used to find the total transmission and reflection measurements. Then section (4.2) uses measurement techniques similar to section (4.1) but with a sample holder. The following section (4.3) describes the measurement technique to determine the external quantum efficiency of the fabricated polymer layers. Finally the section (4.4) describes the setup that enables the measurement of the spectral and angular distribution of the emitted light of the FSLSC.

4.1 Perkin Elmer Lambda 950 Spectrophotometer

The Perkin Elmer Lambda 950 spectrometer enables measurements of total transmission and total reflection of samples. This device is shown in Figure 4.1 [37]. There are two compartments located in the device, which give the user access to a sample compartment and a detector compartment. The sample compartment can only hold cuvettes that contain liquid samples which can be placed in the beam line. When no sample is present in the slot, the light beam just passes through this compartment into the second compartment, the detector compartment, where the integrating sphere is located. This can be seen by the Figure 4.2[38]. The spectrometer makes use of an integrating sphere to capture all of the reflected light. An integrating sphere is a hollow spherical enclosure that is coated with a highly reflective material and two detectors located at the bottom of the sphere to measure the intensity of light. The main purpose of the sphere is to ensures that all the reflected light is randomized before detection, meaning all of the reflected light can be measured. The inner wall of the sphere is made from Spectralon, which diffusely reflects 99% of the incoming light. This material ensures homogeneous light distribution throughout the sphere.

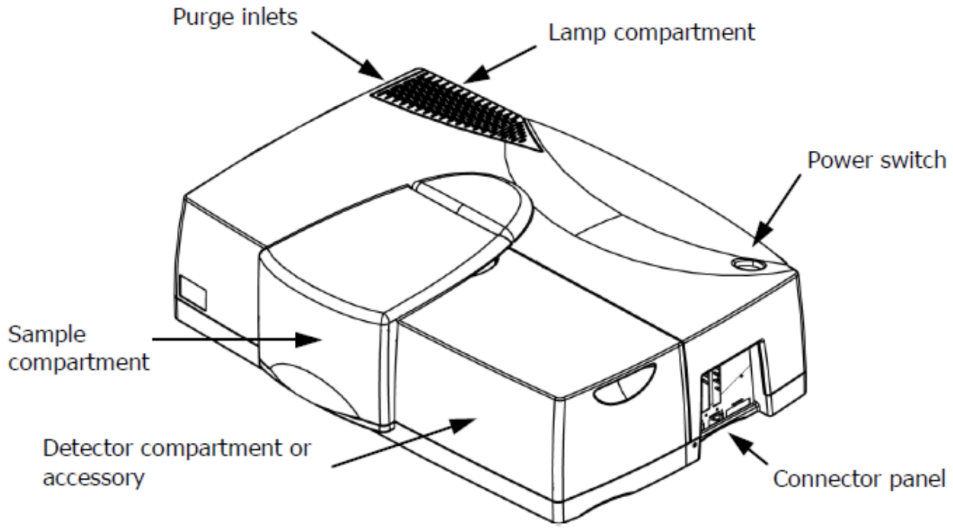

FIGURE 4.1: A overview of Perkin Elmer Lambda 950 Spectrophotometer and its components, referenced from: [37]

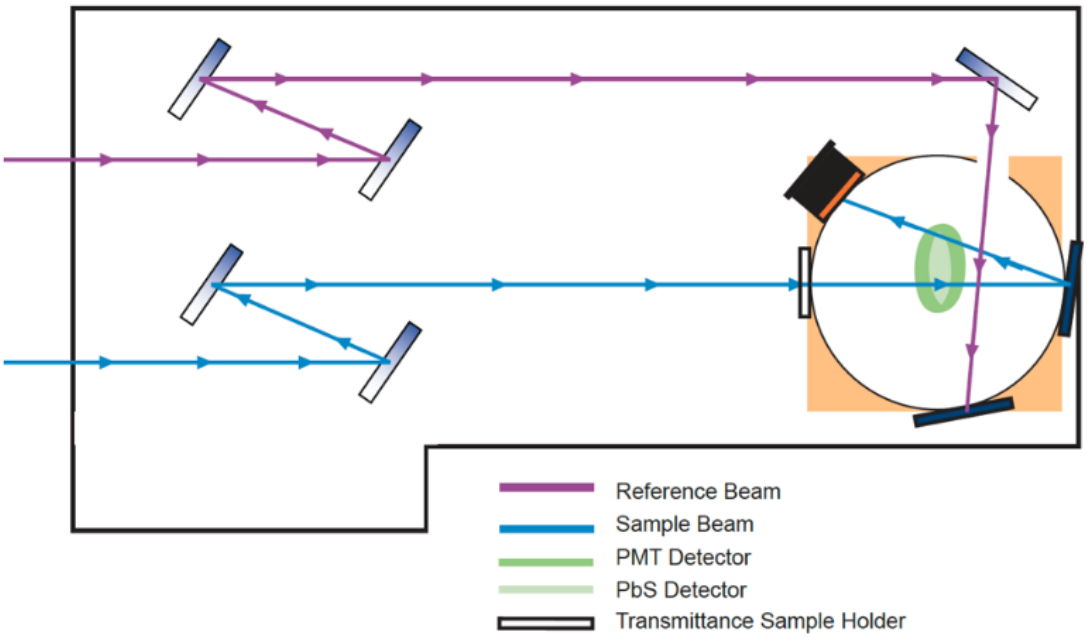

FIGURE 4.2: A schematic view of Perkin Elmer Lambda 950 Spectrophotometer, referenced from: [38]

The integrating sphere has two ports for light to enter. The first entrance port is used for a reference measurement. The reference beam enters through this port. The light which enters is randomized due to multiple diffuse reflections and the measurements are recorded by the detector. The use of the reference beam is to determine the total intensity of the incoming light. Through the other entrance port, light that passes through a sample, is incident and detected by the spectrometer for

transmittance measurements. The output of a measurement is the intensity of the sample beam divided by the intensity of the reference beam. The port at the back of the integrating sphere can be covered by a Spectralon reflection standard. This is done during transmission measurements. Afterwards it is replaced with a sample to measure the reflectance.

The sample beam can be positioned at three spots inside the spectrometer. The first is in the sample cuvette holder that is located 20cm in-front of the transmission port. The second is in the transmission sample holder just outside of the integrating sphere to the left, such that the sample touches the integrating sphere. This is used for total transmission measurements. The last position is at the reflection port, also pressed against the outside of the sphere but to the right of the sphere this time. This is used for reflection measurements. Finally, it can be put in the cuvette holder, which is located about 20cm in front of the transmission port. During a measurement, the spectrometer will sweep over the wavelength range of 175nm to 3300nm. For each wavelength two separate intensity measurements are taken. One for the reference beam and the other for the sample. The transmission and reflectance measurements are taken for all the fabricated polymer layers.

4.2 Perkin Elmer Lambda 950 Spectrophotometer with sample holder

The extent of photoluminescense of the samples needs to be determined. The photoluminescense properties of the polymer layers can be determined by inserting the sample into the integrating sphere. This is done to ensure that all the emitted light is reflected and captured by the detector. A sample holder is used to suspend the sample in the center of the integrating sphere for these measurements. The sample holder can be depicted by the figure 4.3. An issue faced with using this setup to measure the photoluminescense is that the detector of the integrating sphere cannot measure the intensity of the emitted luminescent light. The issue is that only the intensity measured is calibrated per wavelength. The machine is not able to distinguish that the emitted light is of a different wavelength. The polymer layer converts light from lower wavelength to a higher wavelength. When the detector checks for light at the lower wavelength, it cannot measure the light of higher wavelength which are emitted by the luminophore. To resolve this issue another setup is designed which is explained in the next section.

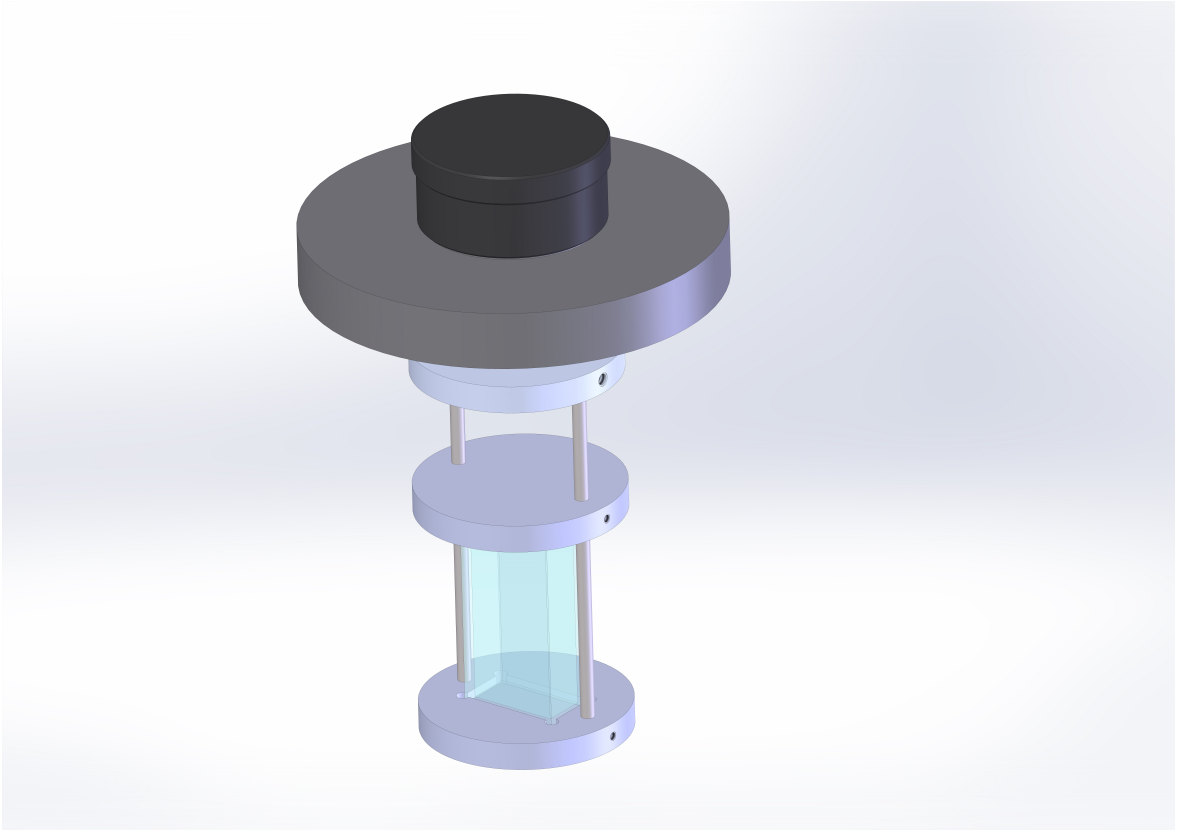

FIGURE 4.3: Sample holder used for photoluminescense in the integrating sphere

4.3 Integrating sphere with sample holder

This section explains the determination of the photoluminescense external quantum efficiency (PLQE) of the solid polymer layers and liquid dye used for comparison. This can be accomplished by using the sample holder which is placed inside the integrating sphere, a separate monochromatic light source and a calibrated fiber-coupled spectrometer. The spectrometer is calibrated by the manufacturer such that it measures the intensity in [μW/cm2/nm].
The photoluminescence in liquids are relatively simple due to isotropic angular distribution of the emission [39]. But for thin solid films this is not the case. For molecular and polymeric materials, anisotropy in the distribution of chromophores leads to an anisotropy in the emission dipole-moment [39]. Also the angular distribution of the emission is altered due to the waveguide effect of the solid polymer layer. To overcome this hurdle, the exact photoluminescence can be determined by taking three different types of measurements. The basic experiment setup is shown in figure 4.4.

The laser enters from the left of the integrating sphere, where the sample holder is kept. A spectrometer is placed outside next to the laser light source to measure

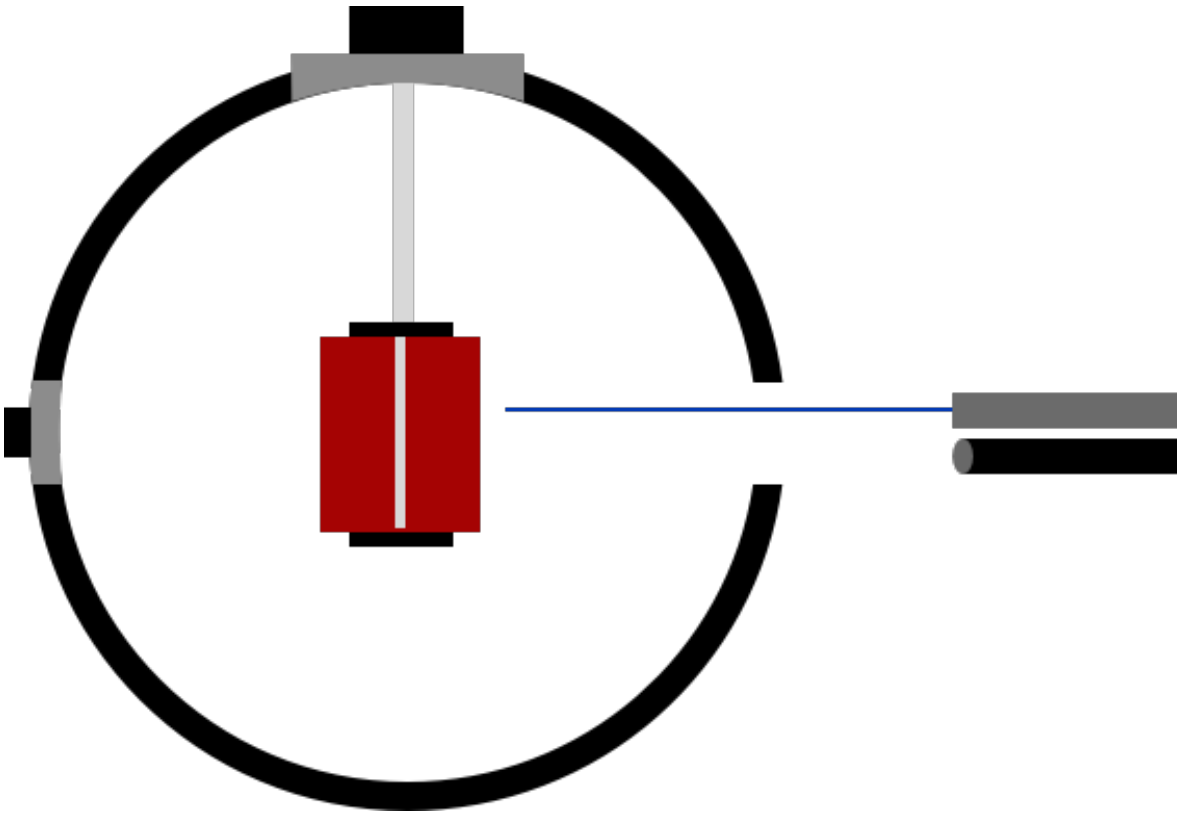

FIGURE 4.4: Basic experiment setup for measuring PLQE of solids

the emission values. As mentioned earlier three different types of measurements are required. For the first measurement, the integrating sphere is empty without a sample and the intensity of the laser that is reflected is recorded. For the second measurement the sample is placed inside the integrating sphere and the laser is made to strike the walls of the integrating sphere. Light is reflected off the walls and then absorbed by the sample. In the third measurement, the sample is placed inside the integrating sphere and the laser is made to strike the sample directly. The sample is oriented in such a way that the laser reflected from the surface of the sample is directed onto the sphere walls and not allowed back though the entrance hole. The measurements are taken for the samples and the intensity of light is recorded. Figures 4.5, 4.6, 4.7 depict the three measurement methods mentioned above. These experiments are carried out with a blue laser of intensity 10.78 mW as well as a green laser of intensity 5 mW. This is performed to test how the polymer layer responds to the light source.

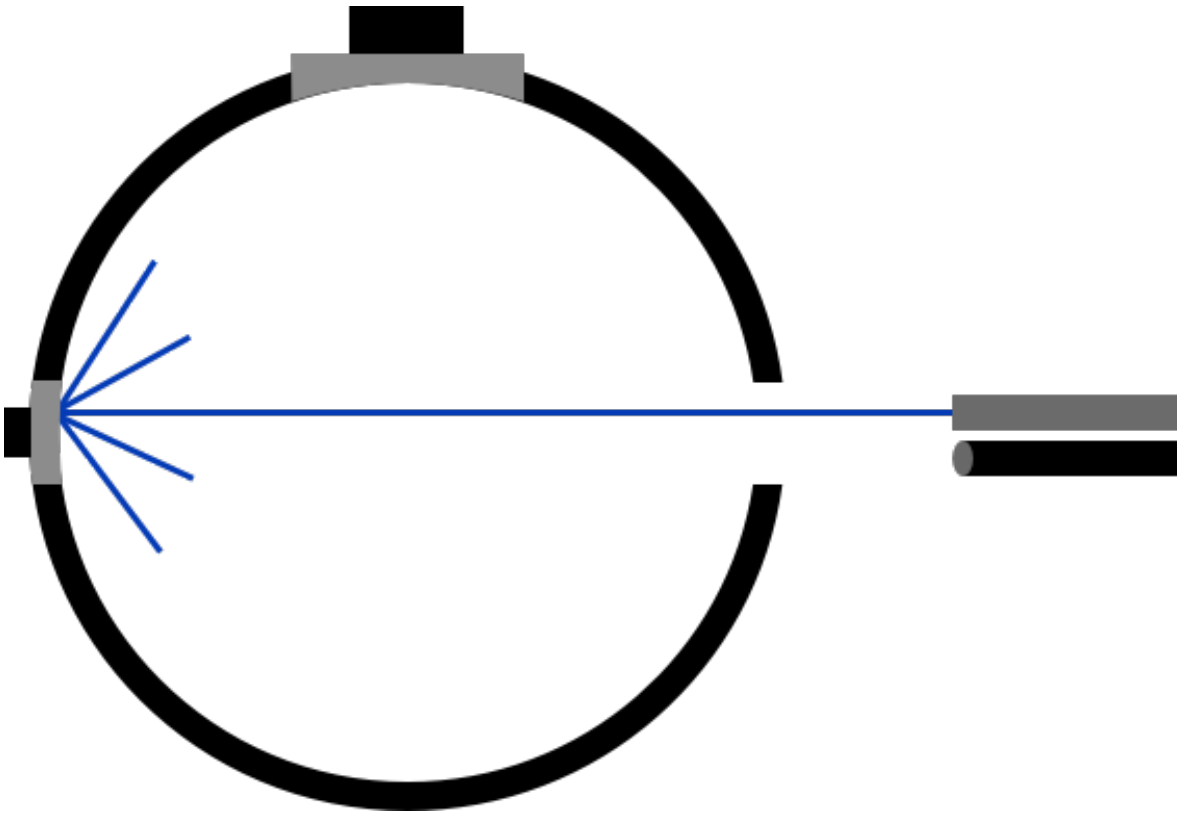

FIGURE 4.5: Experiment with no sample

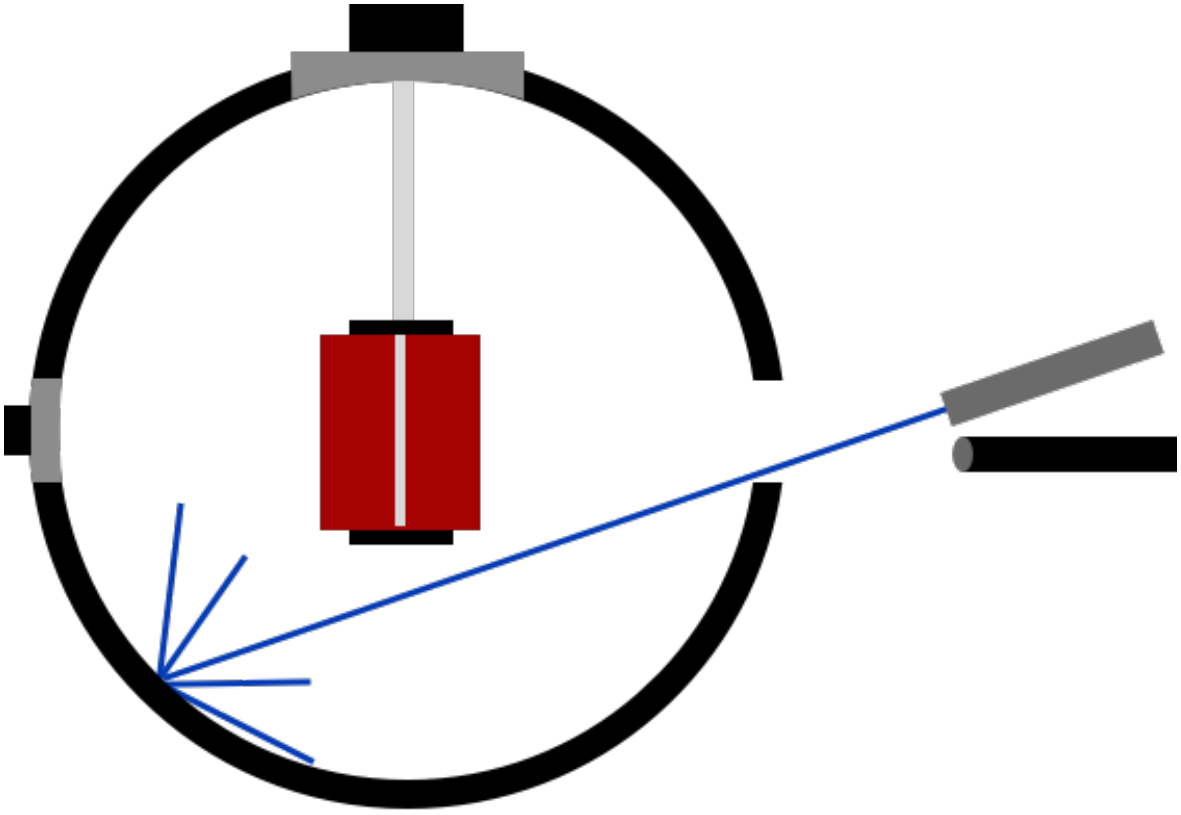

FIGURE 4.6: Experiment with sample laser light strikes walls

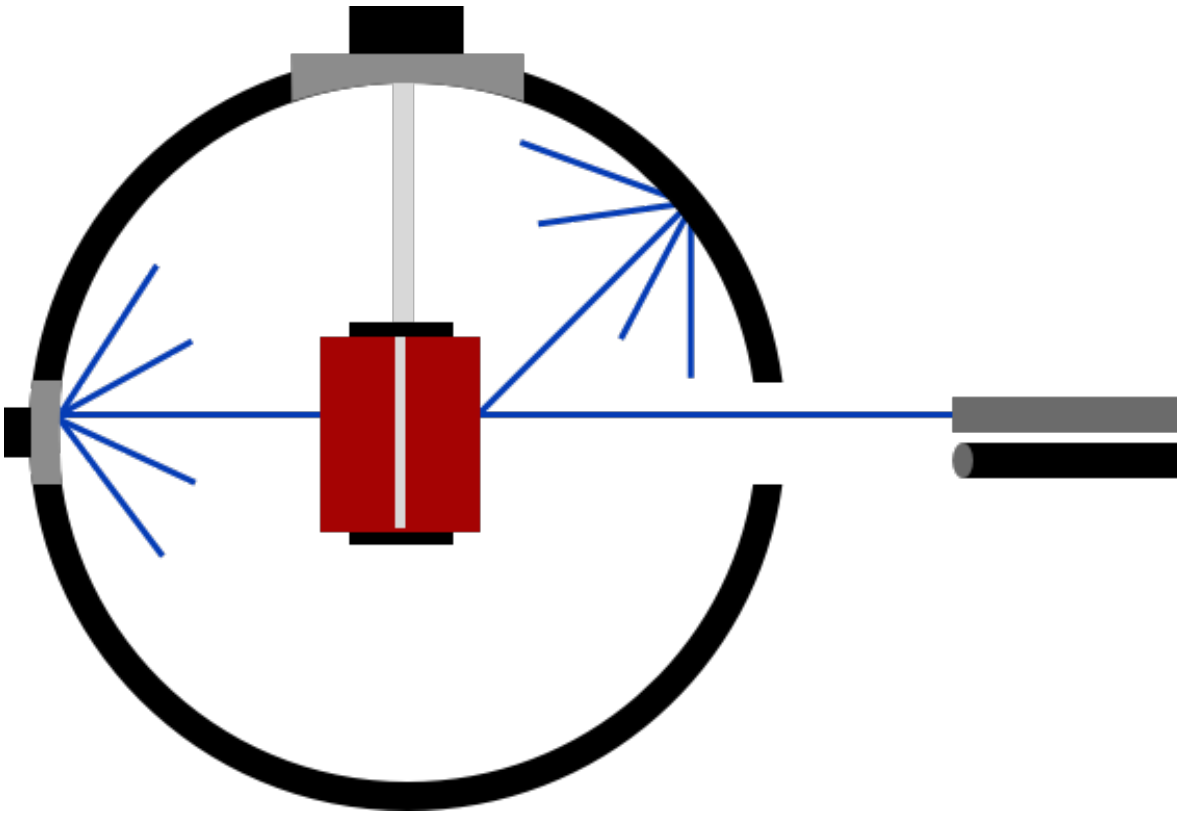

FIGURE 4.7: Experiment with sample and laser light directly striking the sample

4.4 Spectro angular measurements

In order to evaluate the performance of the FSLSC, its output needs to be measured as a function of the emission angle. This can be achieved by using a spectrometer which moves in a circle around the sample. A top-down view is shown schematically in Figure 4.8. A calibrated fiber-coupled spectrometer, which uses a grating to split the light and a CMOS to determine the intensity at each wavelength which is measured. A cosine corrector is attached to the end of the fiber. The role of the cosine corrector is to diffuse the incoming signal, which reduces the dependence of the signal on the fiber orientation. This also increases the viewing angle of the fiber to 180 degrees.

The spectrometer measures the intensity in [µW/cm2/nm]. This helps with determining the actual energy content and it also makes it possible to calculate the total emitted or reflected power for a diffuse sample.

Assuming azimuthal symmetry of the samples, the reflectance only depends on the angle of detection with respect to the sample's normal. The total emitted power can be calculated from the measured intensities at different angles through a surface integral. This integral is taken over a sphere around the sample with a radius

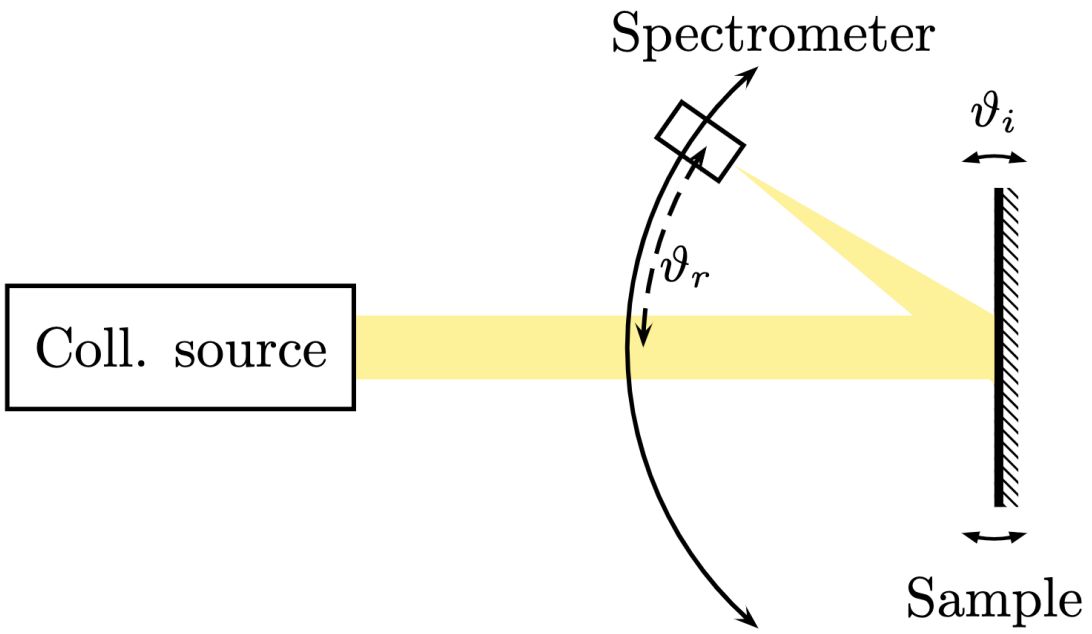

FIGURE 4.8: Schematic set up for the Spectro angular measurements

equal to the detection distance. This measure irradiance M(θ,λ) has the units of μW/cm2/nm]. On integration of this over the reflected spectrum, the total emitted power can be determined.

$$P(\theta) = \int M(\theta, \lambda) d\lambda \tag{4.1}$$

P represents the total power flowing through one square centimetre at a certain distance from the emitter in a certain direction. The total power through a surface integral in spherical coordinates can be calculated[24].

$$P = \int_0^{2\pi} \int_0^{\pi} P(\theta) r^2 sin\theta d\theta d\phi \tag{4.2}$$

Since azimuthal symmetry for the sample is assumed, the outer integral of φ results in a factor of 2π. The detector is able to move around the sample in a complete circle, therefore making the distance to the sample constant. The next step is to measure the power at enough detection angles to get an accurate result for this integral. With the mentioned setup, the angle can be altered in steps size of 10 degrees from 10 to 170 degrees. This results in at most 15 data points, which is enough to accurately evaluate equation 4.2 numerically. The data needs to be extrapolated to determine the total measured power. Since we have a model for the distribution

of the emission, a fit can be made from the amplitude to the data and then integrate the curve obtained.

Chapter 5

Experimental Results

This chapter describes the results obtained from the measurement techniques. The first section 5.1 describes the transmission, reflectance and absorption results obtained by the Perkins Elmer Lambda 950 Spectrometer. The next section 5.2 describes the results obtained using the Perkins Elmer Lambda 950 Spectrometer and the sample holder. The following section 5.3 describes the photoluminescent external quantum efficiency. Finally in section 5.4 the results of emission distribution profile is discussed.

5.1 Results of Perkin Elmer Lambda 950 Spectrophotometer

The transmittance and reflectance is measured for all the fabricated samples using the Perkin Elmer Lambda 950 Spectrophotometer and the absorption was calculated. The Absorption obtained should follow Lambert-Beer law. The wavelength dependent absorption should follow equation 5.1

$$A(\lambda) = 1 - e^{-\alpha(\lambda)L} \tag{5.1}$$

First the transmission and the reflectance for all the fabricated samples are measured. The change in transmission values in this scenario is mainly due to absorption by the luminophores. In figure 5.1 the transmission measurements for the 4 layers with varying concentrations is shown. In figure 5.2 the reflectance measurements for the 4 layers with varying concentrations are depicted and in figure 5.3 the absorption for the 4 layers with varying concentrations are calculated. The total light passing through a system is given by the material's property to transmit a portion of light, to reflect light and to absorb it. The absorption is calculated from the equation 5.2.

$$Absorption = 100 - (Transmission + Reflection) \tag{5.2}$$

The remaining measurements can be found in the appendix 8.2.1, 8.2.2, 8.2.3 for transmission measurements, reflection measurements and absorption respectively. When keeping the concentration of PMMA constant and increasing the Lumogen dye concentration, the absorption of light of lower wavelength is increased with increasing concentration. With each concentration of PMMA i.e. 3.3% (2 layers, 3 layers, 4 layers, 5 layers, 6 layers), 10%, 15%, 20%, 30%, it is observed that with increasing concentration of the dye (i.e. 38.10 PPM, 74.16 PPM, 119.33 PPM, 171.56 PPM, 219.64 PPM) the absorbance also increases. By increasing the PMMA concentration, the amount of absorption does not change. This is due to the fact that the lumogen dye concentration remains the same.

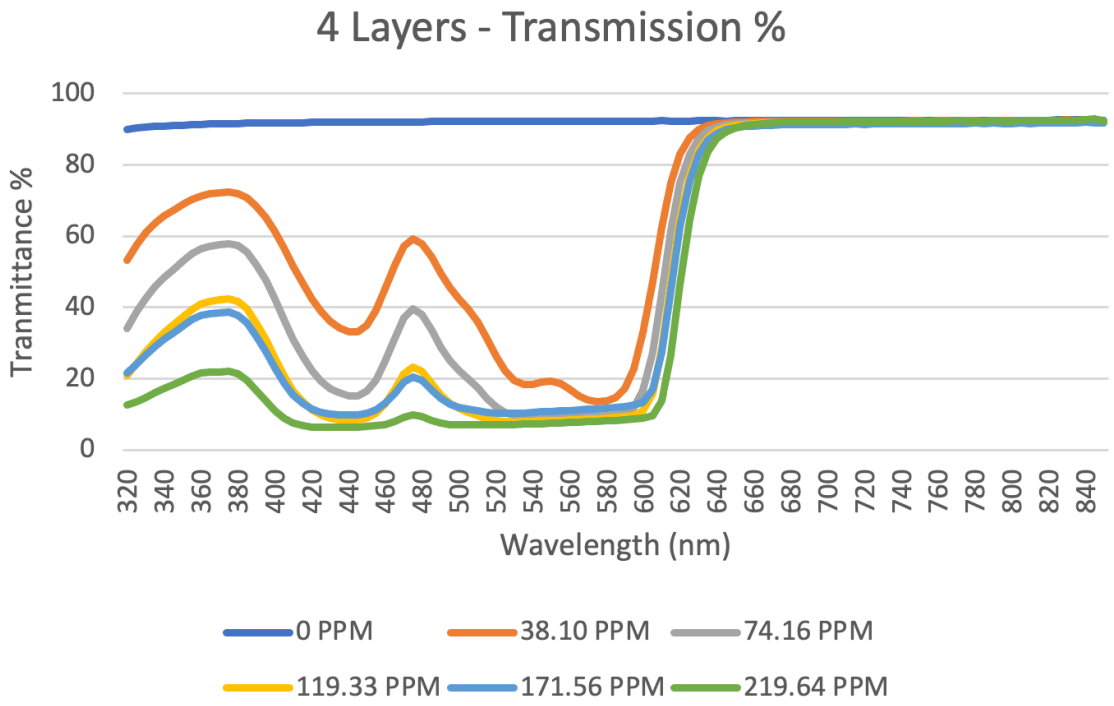

FIGURE 5.1: Transmission results of 4 layers of polymer layer infused with Lumogen f red 305 measured on Perkin Elmer Lambda 950 Spectrophotometer

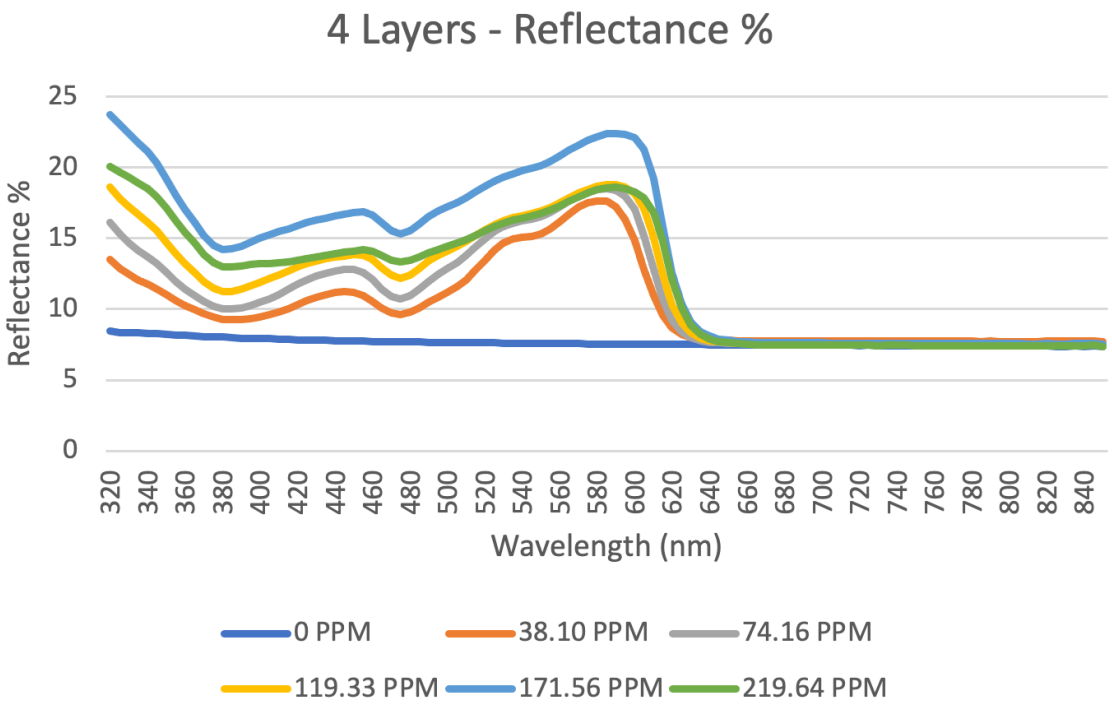

FIGURE 5.2: Reflectance results of 4 layers of polymer layer infused with Lumogen f red 305 measured on Perkin Elmer Lambda 950 Spectrophotometer

5.1.1 Characterization of Bubbles

When increasing the concentration of PMMA (by weight%), the viscosity of the solution containing PMMA and toluene also increases. This high viscosity leads to issue when drying. Since all the volatile solvent is removed from the system by evaporation, the high viscosity led to formation of bubbles while drying. The figure 5.4 depicts the effect of bubbles on the absorption. The sample without bubbles transmits a higher amount of light, when compared to a sample with bubbles.

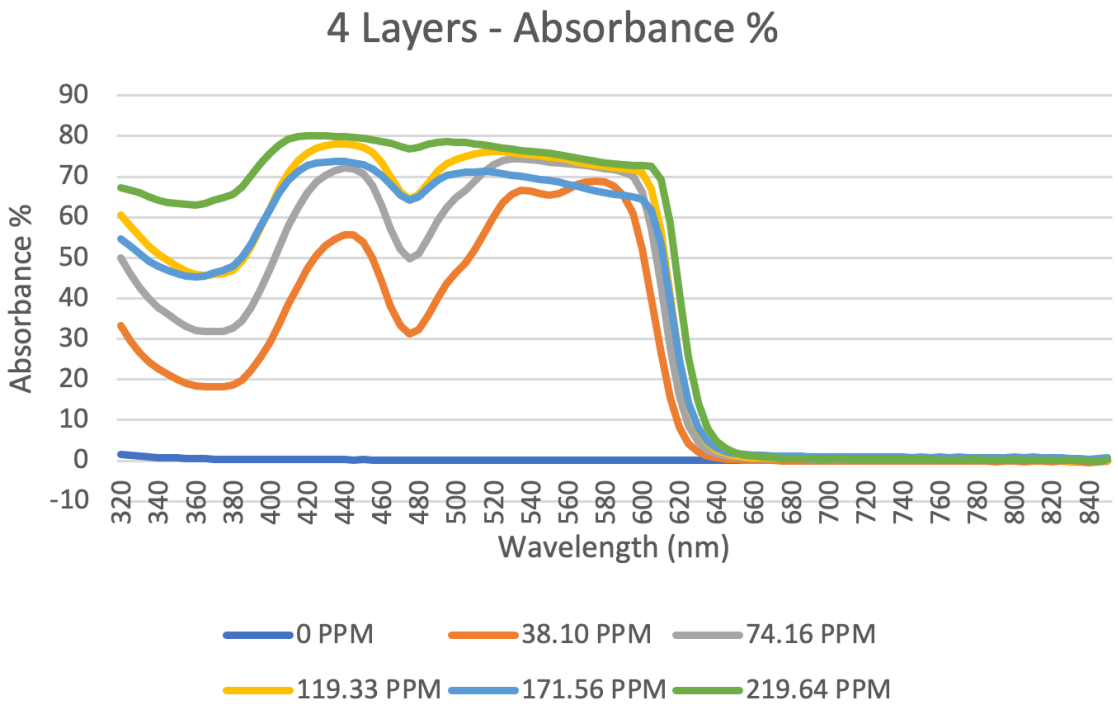

FIGURE 5.3: Absorption results of 4 layers of polymer layer infused with Lumogen f red 305 calculated using tranmission and reflectance measurements

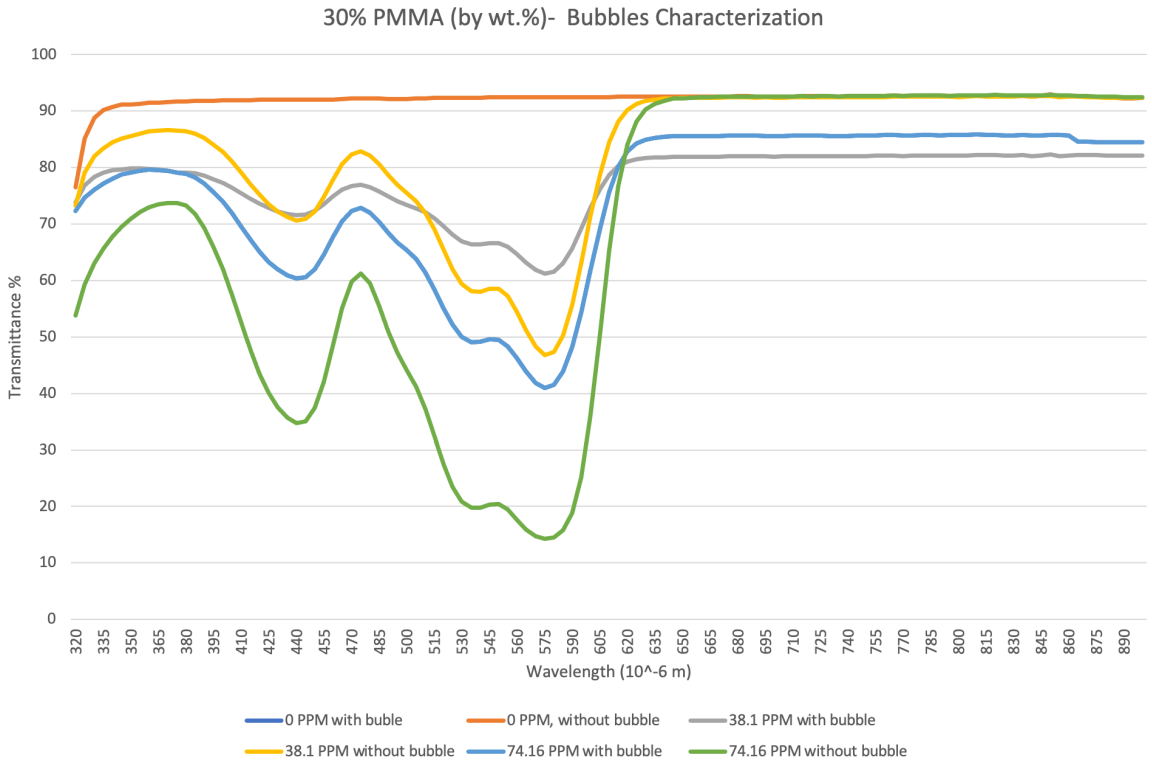

FIGURE 5.4: Characterization of bubbles in polymer layer

5.2 Results of Perkin Elmer Lambda 950 Spectrophotometer with sample holder

When using the sample holder in the integrating sphere, it is possible to capture all the emitted light by the polymer layer infused with the lumogen dye. But as mentioned in the earlier section 4.2 the Perkin Elmer Lambda 950 Spectrophotometer is not able to distinguish, if emitted light is of a different wavelength. The detector when checking for the lower wavelengths of light cannot measure the light of higher wavelength which is emitted by the polymer layer containing the lumogen red dye. This phenomenon is observed in the following figure 5.5.

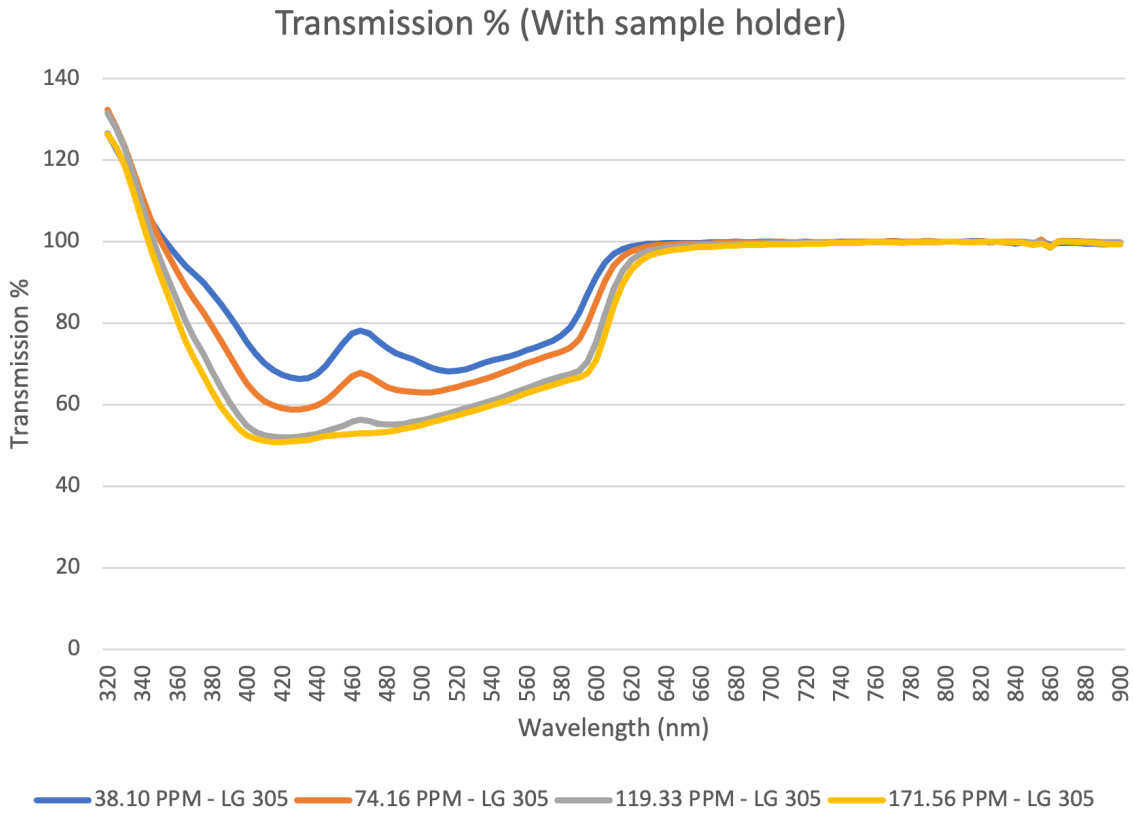

FIGURE 5.5: Transmission results of Perkin Elmer Lambda 950 Spectrophotometer with sample holder

5.3 Results of integrating sphere with sample holder / Photoluminescent external quantum efficiency

This section depicts how the photoluminescent external quantum efficiency is measured. The photoluminescent external quantum efficiency can be attained by performing the three types of measurements mentioned in section 4.2. When light hits the integrating sphere in the absence of the sample (figure 4.5), the laser light gets diffuse and is reflected. With this measurement the total intensity of light entering the integrating sphere is recorded. The following figure 5.6 gives the recorded intensities for the first measurement. The amount of unabsorbed light L_a can be given by the area under the laser curve.

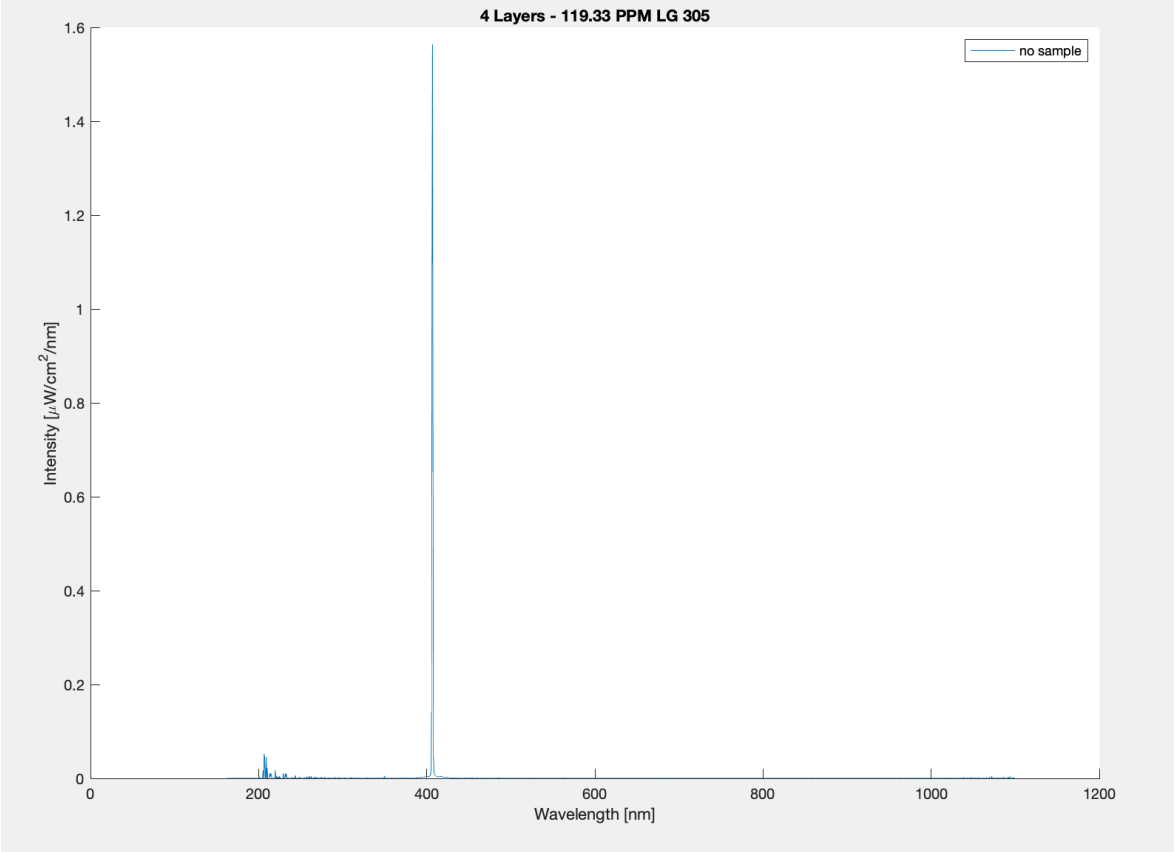

FIGURE 5.6: Figure depicts the measurements that are performed without a sample with blue laser

For the second measurement, when a sample is placed inside the integrating sphere and the laser is directed onto the walls of the integrating sphere, the laser light is scattered from the sphere walls and then strikes the sample. The sample absorbs a fraction of the reflected diffuse light μ and is absorbed by the sample (figure 4.6). The following figure 5.7 gives the recorded intensities for the second measurement. The amount of unabsorbed light L_b can be given by the area under the laser

curve and P_b gives the emitted light due to a fraction of light being absorbed. The amount of light unabsorbed in the second measurement can be given by the following equation 5.3.

$$L_b = L_a(1 - \mu) \tag{5.3}$$

The detected light in this measurement consists of scattered laser light and light emitted due to absorption of scattered laser light. The number of photons which strike the detector is given by $L_b + P_b$.

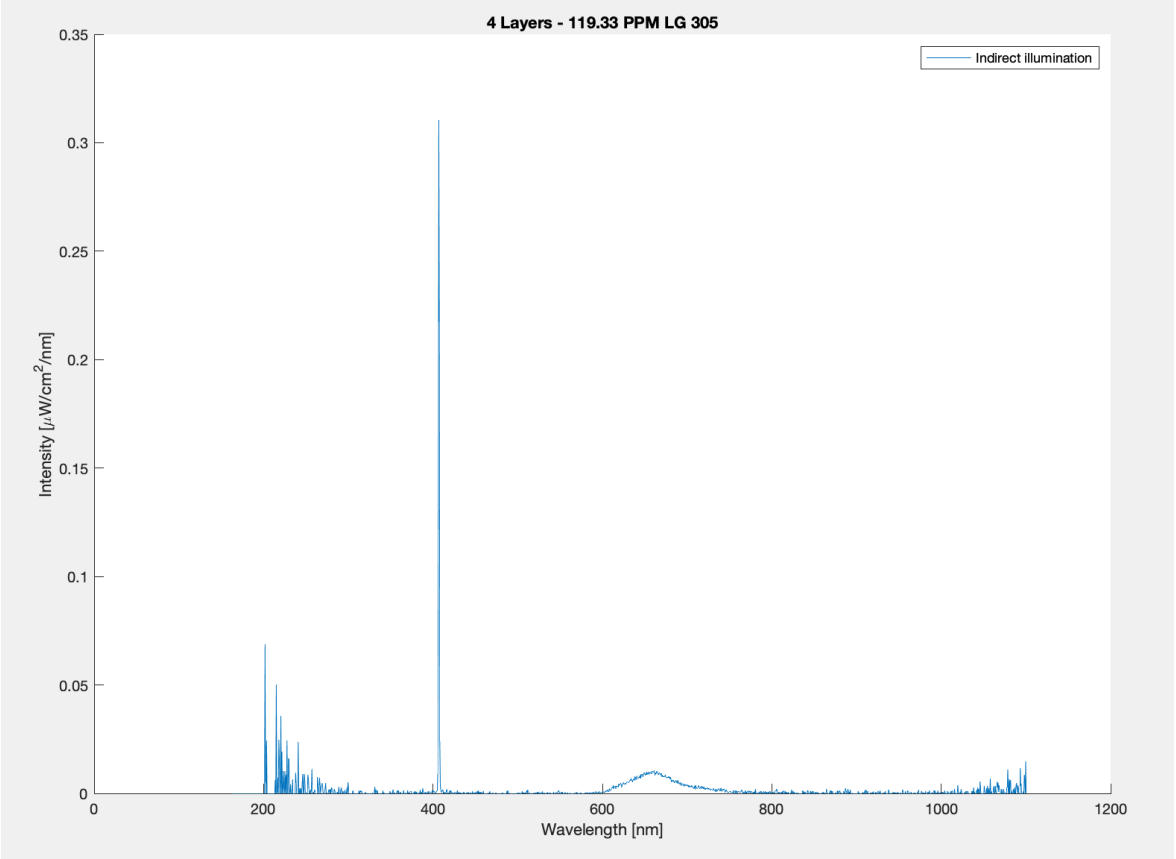

FIGURE 5.7: Figure depicts the measurements that are performed with sample hitting the walls of the integrating sphere with blue laser

In the third measurement when the laser light strikes the sample directly (figure 4.7), a fraction 'A', of the incident laser light will be absorbed by the sample and a fraction '(1-A)' will be either transmitted or reflected. The unabsorbed light is reflected back onto the interior surface of the integrating sphere where it is scattered. A fraction μ, of this scattered light is absorbed by the sample. The following figure 5.8 gives the recorded intensities for the third measurement.

The amount of unabsorbed light L_c, can be given by the area under the laser curve and P_c gives the emitted light because light is being absorbed. The amount of

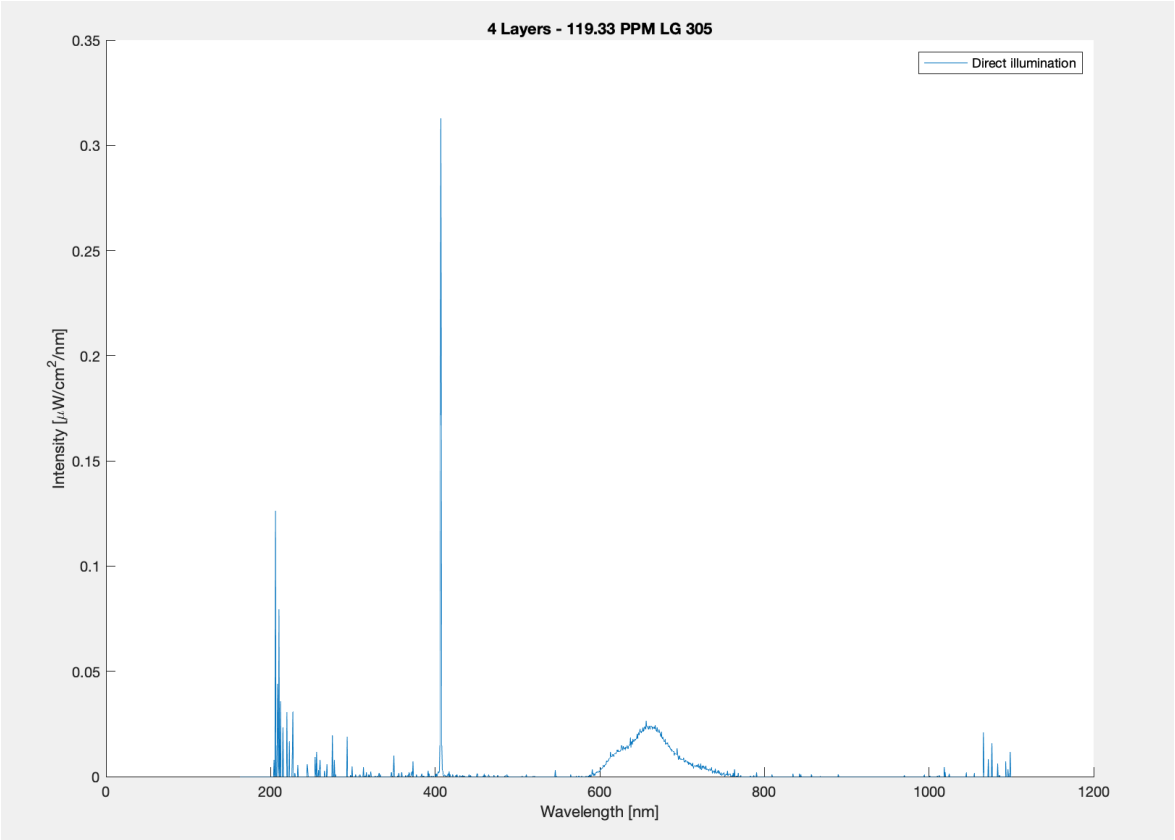

FIGURE 5.8: Figure depicts the measurements that are performed with sample hitting the sample directly with blue laser

light unabsorbed in the third measurement can be given by the following equation 5.4,

$$L_c = L_a(1 - A)(1 - \mu) \tag{5.4}$$

The absorption coefficient can be given by the equation 5.5,

$$A = \frac{L_c}{L_b} \tag{5.5}$$

Now the contribution of scattered light in the third experiment can be given by the equation 5.6.

$$S_l = (1 - A)(L_b + P_c) \tag{5.6}$$

The light emitted due to absorption of collimated laser light is given by the equation 5.7.

$$E_l = (\eta.L_a.A) \tag{5.7}$$

The total intensity over the whole spectrum for the third experiment can be given by the equation 5.9

$$L_c + P_c = S_l + E_l \tag{5.8}$$

$$L_c + P_c = (1 - A)(L_b + P_c) + (\eta L_a A) \tag{5.9}$$

Rearranging the equation the photoluminescent external quantum efficiency can be given by the equation 5.10,

$$\eta = \frac{P_c - (1 - A)P_b}{L_a A} \tag{5.10}$$

The photoluminescent external quantum efficiency for the samples ranging from 2 to 6 layers of polymer layer infused with varying concentrations of lumogen dye, are calculated and are depicted in figure 5.9 for blue laser and figure 5.10 for the green laser. The same is done for the liquid sample which consists of lumogen red dye and toluene, which are prepared to check for their photoluminescence external quantum efficiency. The PLQE for the liquid samples which is depicted in figure 5.11.

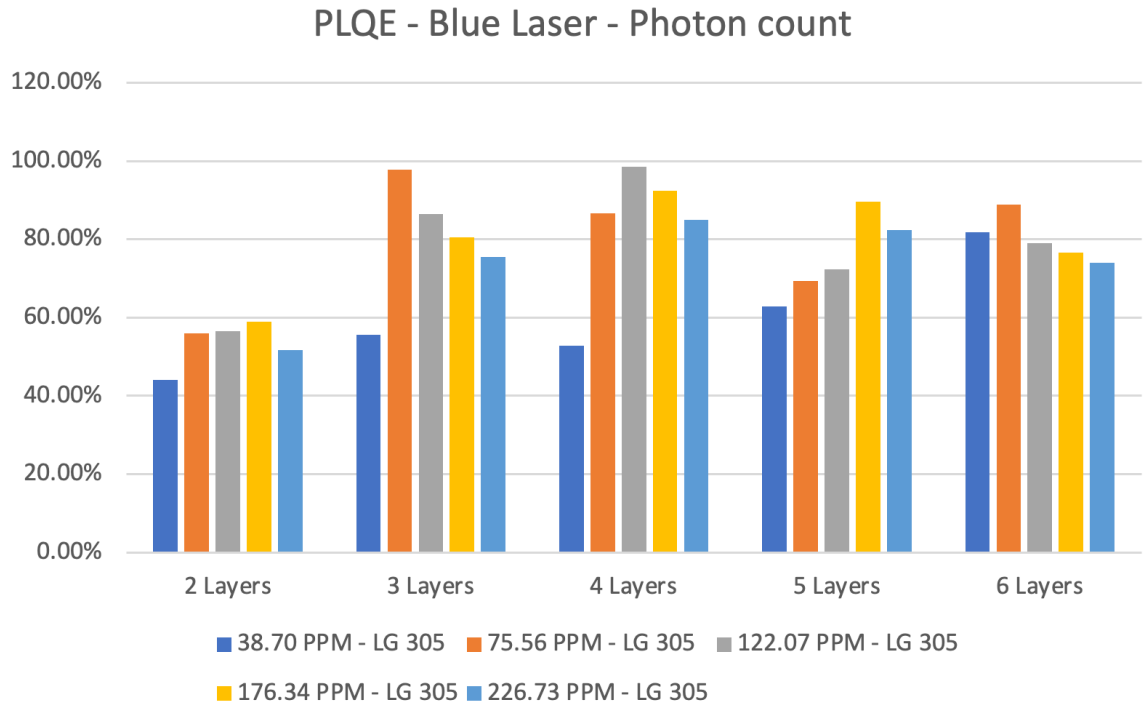

FIGURE 5.9: Figure depicts the photoluminescent external quantum efficiency of solid polymer layer with blue laser excitation

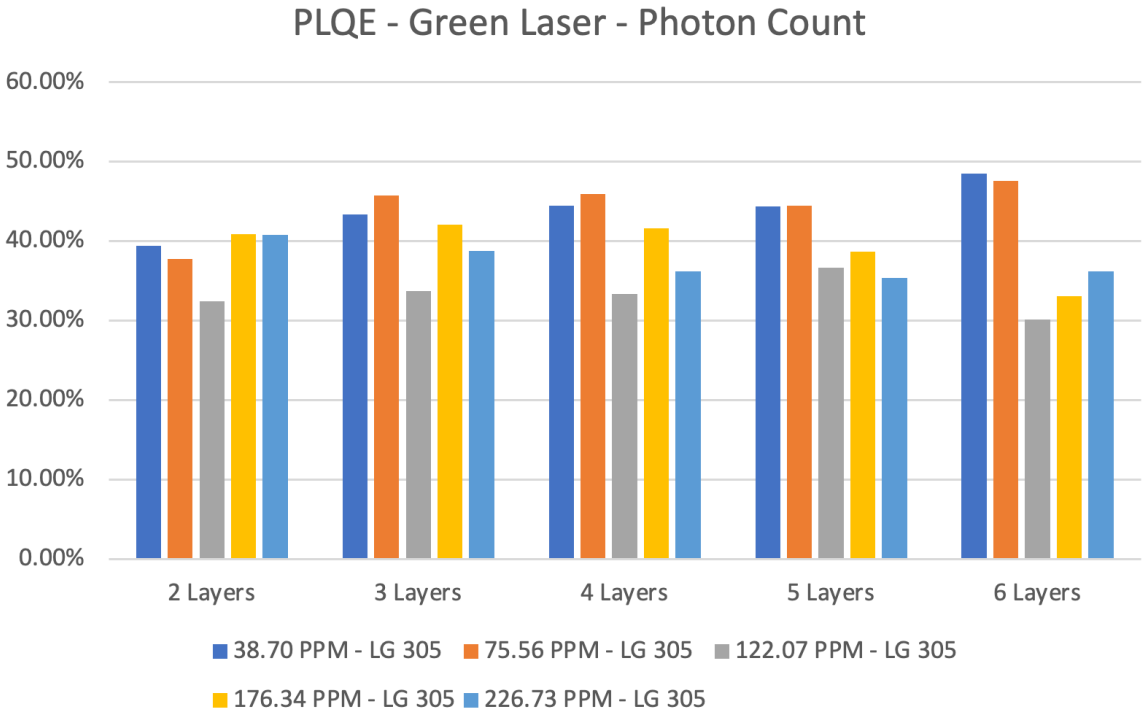

FIGURE 5.10: Figure depicts the photoluminescent external quantum efficiency of solid polymer layer with green laser excitation

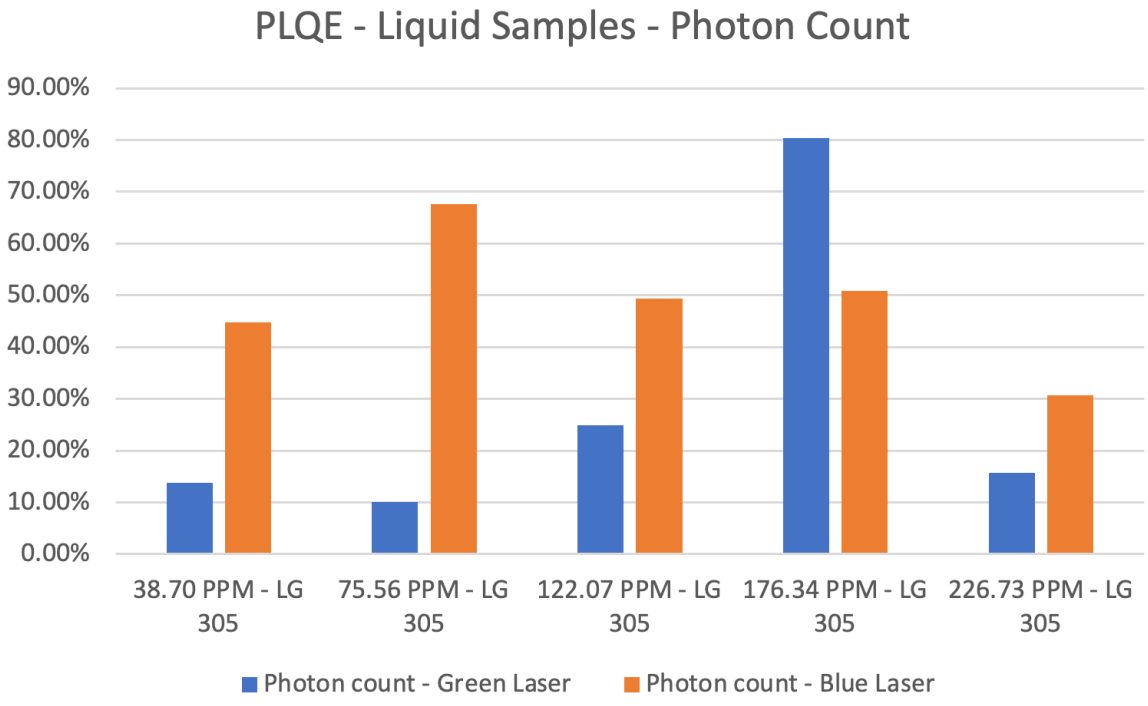

FIGURE 5.11: Figure depicts the photoluminescent external quantum efficiency of Liquid polymer layer with blue, green laser excitation

An observation can be made that the PLQE for the wafers embedded with lumogen for PMMA concentration of 3.3% with varying dye concentrations follow a similar trend when illuminated with a blue laser. With the increasing layers, the concentration of lumogen dye and PMMA is the same, but the thickness of the polymer layer increases. For each polymer layer with 3.3% PMMA concentration and increasing layer thickness a similar trend is observed for the PLQE. There is an increase of PLQE till a certain concentration and then it decreases. The highest photoluminescent external quantum efficiency of solid polymer layers was observed by the blue laser excitation of 98% in the 4 layers (3.3% PMMA by wt%) with concentration of 119.33 PPM. When increasing the concentration of PMMA and keeping the dye concentration constant, the photoluminescent external quantum efficiency follows a similar trend but the efficiencies are lower. The conversion efficiency of blue laser light is higher than the green light. The blue laser has a higher intensity therefore a higher conversion efficiency. When increasing the thickness of the polymer layer, the PQLE increases but it decreases after reaching 4 layers, as the re-absorption in the layers increase. When the dye is suspended in a liquid medium, the photoluminescent external quantum efficiency is lowered with a max conversion of 80% for the sample with concentration of 176.34 PPM when illuminated with green laser. However, the PLQE trend observed for the polymer layers (3.3% PMMA by wt%) with increasing concentration of lumogen dye with the green laser is not the same as with blue laser. The absorption of light by the dye is different for the blue laser and green laser source.

5.4 Emission distribution profile / Specto-Angular Measurements

In this section the results of the measurements performed with the spectro angular setup are discussed. The measurements are performed for the prototype of the FSLSC module. The spectrometer used is calibrated to measure intensity of light at all wavelengths. The intensity (power per area) of the emitted light can be converted to radiance based on the distance between the sample and the detector. Therefore the recorded intensity by the spectrometer is proportional to the intensity emitted by the FSLSC module. Hence, the plot represented in this section will depict the intensity by the spectrometer. The conversion to radiance only matters in the calculations of the total power as shown in equation 4.2.

The first measurement is performed with the FSLSC containing the polymer layer with 4 Layers and concentration of 119.33 PPM Lumogen dye. The second

measurement had the FSLSC with 4 layers and concentration of 171.56 PPM and finally the third measurement included the FSLSC with 6 layers and a concentration of 38.70 PPM Lumogen dye, a third measurement with the FSLSC and concentration of 119.33 PPM Lumogen dye. Lastly for a reference comparison, the spectro-angular measurements are taken for a Lambertian reflector. The module is placed on the sample holder and the light from the spectral source is normally incident on it. The lamp is aligned as such that the module is completely illuminated by light. Measurements are made taken from 10°as the spectrometer is blocked by the setup. The measurements are taken in step sizes of 10°. The measurements are shown in the figure 5.12. There are lower values for for the point of 80°and 90°, as there is a shadow cast by the spectrometer on the sample. It can be observed the polymer layer with 6 layers with a concentration of 38.70 PPM Lumogen dye has the highest area under the curve. The lamp used, consists of a light source that has a wavelength range of 240 nm - 2400 nm and an intensity of 1.3 W. This includes wavelength of blue and green light.

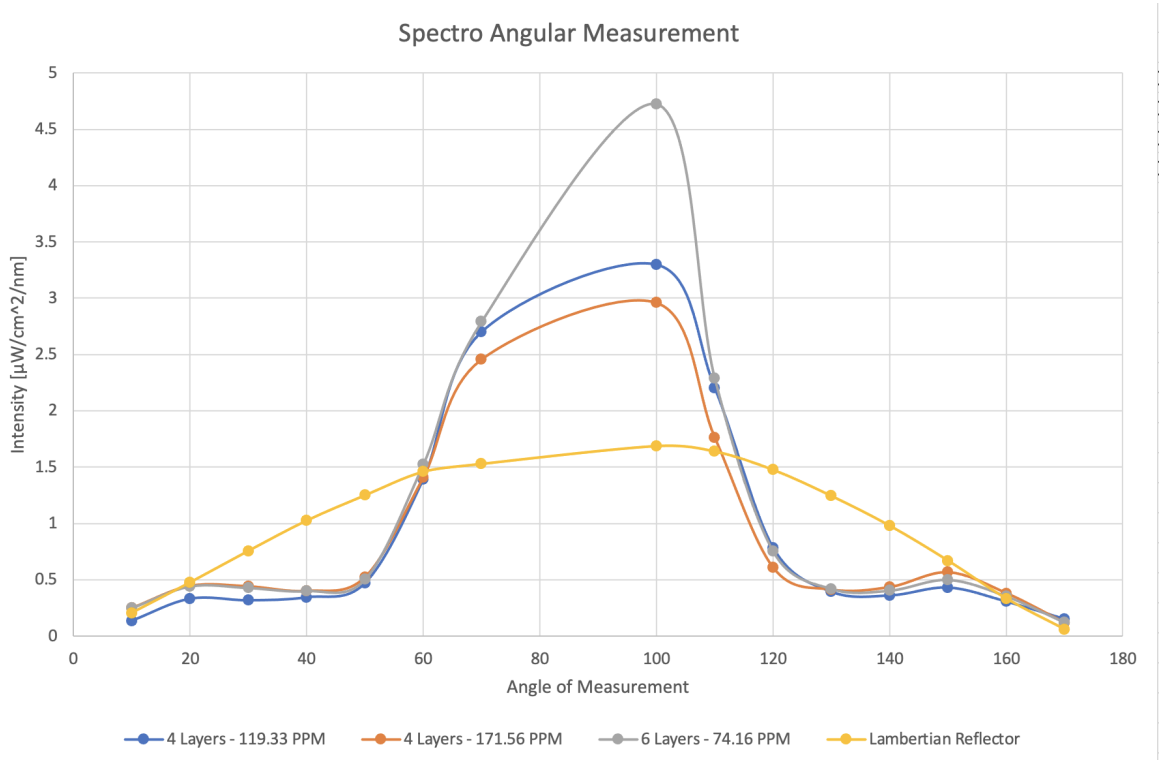

FIGURE 5.12: Figure depicts the total measured emitted intensity by the FSLSC module and a Lambertian reflector

Chapter 6

Conclusion

During this research the polymer layer infused with different concentrations of Lumogen F RED 305 is fabricated for its intended use in the FSLSC. This is done by first synthesising a thin layer with varying concentrations of the lumogen dye. The quantity of the polymer is increased to get thicker layers. Upon altering the PMMA and lumogen dye concentrations, different layers with increasing concentration of PMMA and Lumogen red are fabricated. Then they are measured for their transmission, reflectance and absorption. After this characterization is done, the photoluminescent external quantum efficiency is determined for the polymer layers with blue and green monochromatic laser. The highest photoluminescent external quantum efficiency with the blue laser was found to be around 98% for the 4 layer polymer with concentration of 119.33 PPM. The highest photoluminescent external quantum efficiency with green laser was found to be around 48% for the 6 layer polymer with concentration of 38.10 PPM. While the highest photoluminescent external quantum efficiency for the liquid samples is around 80%. This research proves that by changing the phase from a liquid state to a solid state of the lumogen housing medium, the photoluminescent external quantum efficiency can be further increased.

Chapter 7

Acknowledgements

First of all, I want to thank everyone in the Saive research group for supporting me and the guidance provided for me during my Master Thesis.
I want to thank Shweta Pal for guiding me to understand concepts of the free-space Luminescent Solar Concentrators. I want to thank Jelle Westerhof for aiding me during the measurements of the spectro-angular measurement setup. I want to thank Jian-Yao for his assistance to setup the measurements for the pholuminescent external quantum efficiency. I want to thank Mathis Van de Voorde for helping me perform silinazition of the petri dishes. I also want to thank the rest of the Saive Research group for input on some complicated topics that relate to both of the projects that are being carried out at the moment.
I want to thank the technicians from the IMS group for there help during this project: Ir. Karin van den Nieuwenhuijzen for teaching me how to work safely and effectively in the chemical lab. Ir. Dominic Post for helping out fabricating the sample holder and applying the Lambertion coating.
I want to thank Dr. Rebecca Saive for having me take part in this interesting research project, although my background was in chemical engineering and for giving me the opportunity to continue my research in the field of solar concentrators. I want once again thank Dr. Rebecca Saive for her guidance and and allowing me to utilize my previous work experience in a relatively new field of study for me.
Finally, I want to thank Prof. Dr. Ir. Andre Ten Elshof and Dr. Dipl.-Ing. for serving as the internal and external member of my committee.

Bibliography

[1] Dolf Gielen et al. “The role of renewable energy in the global energy transformation”. In: *Energy Strategy Reviews* 24 (2019), pp. 38–50.

[2] Sven Rühle. “Tabulated values of the Shockley–Queisser limit for single junction solar cells”. In: *Solar energy* 130 (2016), pp. 139–147.

[3] Kunta Yoshikawa et al. “Exceeding conversion efficiency of 26% by heterojunction interdigitated back contact solar cell with thin film Si technology”. In: *Solar Energy Materials and Solar Cells* 173 (2017), pp. 37–42.

[4] Md Tasbirul Islam et al. “A comprehensive review of state-of-the-art concentrating solar power (CSP) technologies: Current status and research trends”. In: *Renewable and Sustainable Energy Reviews* 91 (2018), pp. 987–1018.

[5] Shweta Pal and Rebecca Saive. “Experimental study of the spectral and angular solar irradiance”. In: *2019 IEEE 46th Photovoltaic Specialists Conference (PVSC)*. IEEE. 2019, pp. 3182–3186.

[6] Harald Ries. “Thermodynamic limitations of the concentration of electromagnetic radiation”. In: *JOSA* 72.3 (1982), pp. 380–385.

[7] Russell J Beal, Barrett G Potter, and Joseph H Simmons. “Angle of incidence effects on external quantum efficiency in multicrystalline silicon photovoltaics”. In: *IEEE Journal of Photovoltaics* 4.6 (2014), pp. 1459–1464.

[8] Blaz Kirn, Kristijan Brecl, and Marko Topic. “A new PV module performance model based on separation of diffuse and direct light”. In: *Solar Energy* 113 (2015), pp. 212–220.

[9] Michael G Debije and Vikram A Rajkumar. “Direct versus indirect illumination of a prototype luminescent solar concentrator”. In: *Solar Energy* 122 (2015), pp. 334–340.

[10] Willes H Weber and John Lambe. “Luminescent greenhouse collector for solar radiation”. In: *Applied optics* 15.10 (1976), pp. 2299–2300.

[11] Wilfried GJHM Van Sark et al. “Luminescent Solar Concentrators-A review of recent results”. In: *Optics express* 16.26 (2008), pp. 21773–21792.

[12] JS Batchelder, AH Zewai, and T Cole. "Luminescent solar concentrators. 1: Theory of operation and techniques for performance evaluation". In: *Applied Optics* 18.18 (1979), pp. 3090–3110.

[13] Lenneke H Slooff et al. "A luminescent solar concentrator with 7.1% power conversion efficiency". In: *physica status solidi (RRL)–Rapid Research Letters* 2.6 (2008), pp. 257–259.

[14] Mark Portnoi et al. "All-silicone-based distributed Bragg reflectors for efficient flexible luminescent solar concentrators". In: *Nano Energy* 70 (2020), p. 104507.

[15] Wouter Eggink and Angèle Reinders. "Design it with LSCs; an exploration of applications for Luminescent Solar Concentrator PV technologies". In: *2017 IEEE 44th photovoltaic specialist conference (PVSC)*. IEEE. 2017, pp. 2109–2113.

[16] AJ Chatten et al. "Quantum dot solar concentrators". In: *Semiconductors* 38.8 (2004), pp. 909–917.

[17] Sahar Saeidi et al. "Efficiency improvement of luminescent solar concentrators using upconversion nitrogen-doped graphene quantum dots". In: *Journal of Power Sources* 476 (2020), p. 228647.

[18] Francesco Meinardi et al. "Large-area luminescent solar concentrators based on 'Stokes-shift-engineered'nanocrystals in a mass-polymerized PMMA matrix". In: *Nature Photonics* 8.5 (2014), pp. 392–399.

[19] Duncan C Wheeler et al. "Semi-Transparent Solar Cell enabled by Frequency Selective Light Trapping". In: *arXiv preprint arXiv:1802.01645* (2017).

[20] Abdelfateh Kerrouche et al. "Luminescent solar concentrators: From experimental validation of 3D ray-tracing simulations to coloured stained-glass windows for BIPV". In: *Solar Energy Materials and Solar Cells* 122 (2014), pp. 99–106.

[21] Michael D Hughes, Duncan E Smith, and Diana-Andra Borca-Tasciuc. "Performance of wedge-shaped luminescent solar concentrators employing phosphor films and annual energy estimation case studies". In: *Renewable Energy* 160 (2020), pp. 513–525.

[22] Lisanne Einhaus and Rebecca Saive. "Free-space concentration of diffused light for photovoltaics". In: *2020 47th IEEE Photovoltaic Specialists Conference (PVSC)*. IEEE. 2020, pp. 1368–1370.

[23] Geert C Heres, Lisanne M Einhaus, and Rebecca Saive. "Analytical Model for the Performance of a Free-Space Luminescent Solar Concentrator". In: *2021 IEEE 48th Photovoltaic Specialists Conference (PVSC)*. IEEE. 2021, pp. 1027–1029.

[24] Master Thesis Geert Heres. *Free-space Luminescent Solar Concentrators*.

[25] T Britannica. "Editors of Encyclopaedia". In: *Argon. Encyclopedia Britannica* (2020).

[26] Altuglass PMMA TDS. *ALTUGLAS V129 UVT technical data sheet*.

[27] I Yu Evchuk et al. "Solubility of polymethyl methacrylate in organic solvents". In: *Russian journal of applied chemistry* 78.10 (2005), pp. 1576–1580.

[28] Xueji Zhang et al. "Exposure strategies for polymethyl methacrylate from in situ x-ray absorption near edge structure spectroscopy". In: *Journal of Vacuum Science Technology B: Microelectronics and Nanometer Structures* 13 (Aug. 1995), pp. 1477 –1483. DOI: 10.1116/1.588175.

[29] Jeroen Dobbelaar. "A broadly applicable red dye doped Luminescent Solar Concentrator photo microreactor". In: *Technische Universiteit Eindhoven* (2017).

[30] Lindsay R Wilson et al. "Characterization and reduction of reabsorption losses in luminescent solar concentrators". In: *Applied optics* 49.9 (2010), pp. 1651–1661.

[31] Lindsay R Wilson and Bryce S Richards. "Measurement method for photoluminescent quantum yields of fluorescent organic dyes in polymethyl methacrylate for luminescent solar concentrators". In: *Applied optics* 48.2 (2009), pp. 212–220.

[32] Nils Steinbrück, Martin Könemann, and Guido Kickelbick. "Effect of polysiloxane encapsulation material compositions on emission behaviour and stabilities of perylene dyes". In: *RSC advances* 8.32 (2018), pp. 18128–18138.

[33] BASF. *Safety data sheet, LUMOGEN RED F 305*. URL: https://docplayer.net/82916569-Safety-data-sheet-lumogen-f-red-substance-preparation-and-company-identification-2-hazard-identification.html.

[34] Uwe Sander and BA Wolf. "Solubility of poly (n-alkylmethacrylate) s in hydrocarbons and in alcohols". In: *Die Angewandte Makromolekulare Chemie: Applied Macromolecular Chemistry and Physics* 139.1 (1986), pp. 149–156.

[35] Rebecca L DeRosa, Penny A Schader, and James E Shelby. "Hydrophilic nature of silicate glass surfaces as a function of exposure condition". In: *Journal of Non-Crystalline Solids* 331.1-3 (2003), pp. 32–40.

[36] F Boccafoschi, L Fusaro, and M Cannas. "Immobilization of peptides on cardiovascular stent". In: *Functionalised cardiovascular stents*. Elsevier, 2018, pp. 305–318.

[37] *Elmer-Lambda950 user manual*. URL: https://resources.perkinelmer.com/corporate/cmsresources/images/44-135972bro_009201b_01lambdaaccessories.pdf.

[38] *Elmer-Lambda950 user manual*. URL: https://cmdis.rpi.edu/sites/default/files/UVVis-PerkinElmer-Lambda950-HardwareGuide.pdf.

[39] John C de Mello, H Felix Wittmann, and Richard H Friend. "An improved experimental determination of external photoluminescence quantum efficiency". In: *Advanced materials* 9.3 (1997), pp. 230–232.

[40] *Calculation of Parts-per-Million (PPM)*. URL: https://www.rapidtables.com/math/number/PPM.html.

Chapter 8

Appendix

8.1 Appendix I

appendix1

8.1.1 Calculations for Concentration in PPM

First the densities of the chemicals are obtained from the technical data sheets. The density of Lumogen F RED 305, PMMA and toluene are required. Since the PMMA and the lumogen dye are measured in grams by weight and toluene is measured in the units of volume in mL there needs to be a standard method to measure the quantities. The mass of toluene is obtained using the formula for the density by 8.1

$$Denisty = \frac{Mass}{Volume} \tag{8.1}$$

Once the mass if found for toluene, the concentration in parts per million can be calculated with the following equation 8.2 [40],

$$Concentration(PPM) = \frac{MassOfSolute}{MassOfSolution} * 10^6 \tag{8.2}$$

8.2 Appendix II

8.2.1 Transmission graphs

This section contains all the transmission graphs for the measured samples.

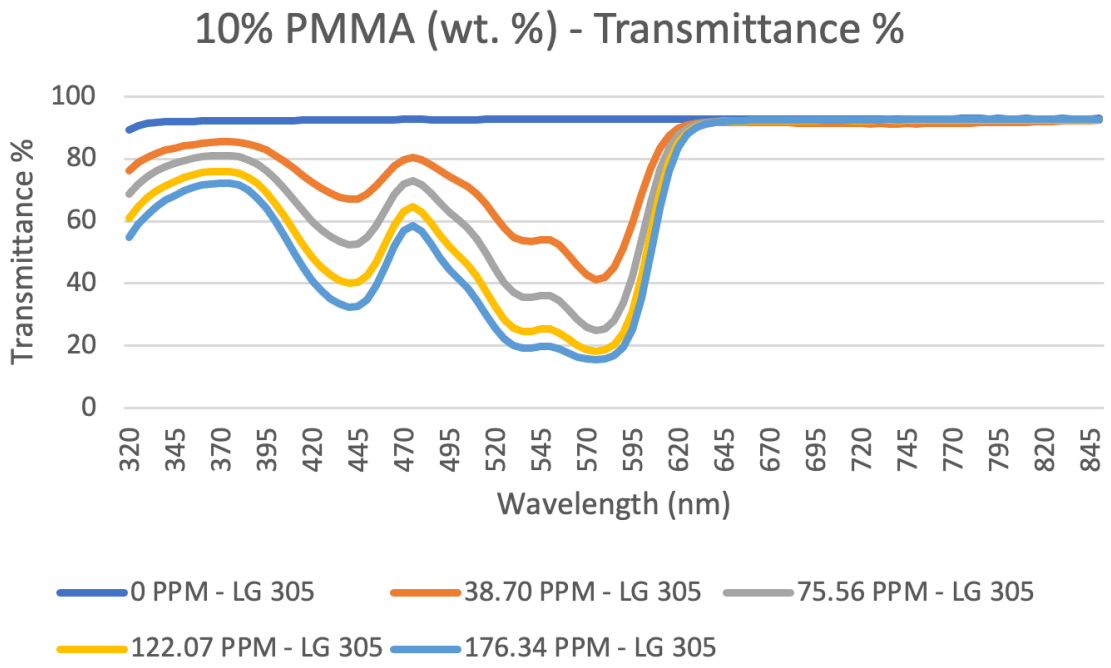

FIGURE 8.1: Transmission results of 10% PMMA infused with Lumogen f red 305 measured on Perkin Elmer Lambda 950 Spectrophotometer

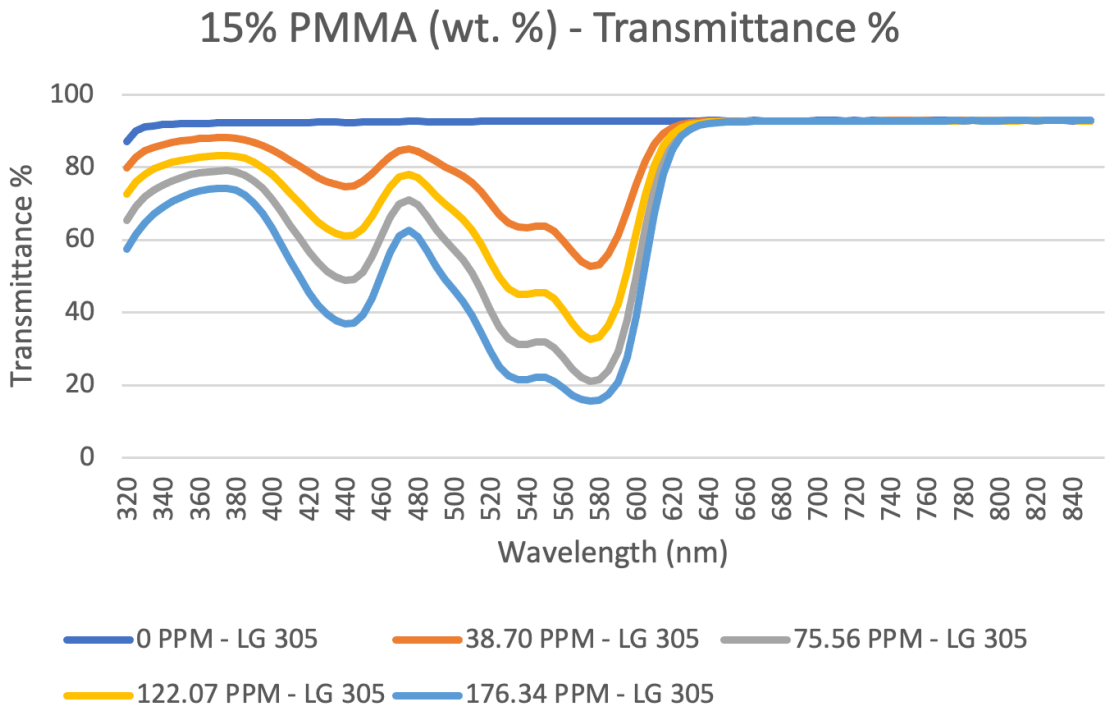

FIGURE 8.2: Transmission results of 15% PMMA infused with Lumogen f red 305 measured on Perkin Elmer Lambda 950 Spectrophotometer

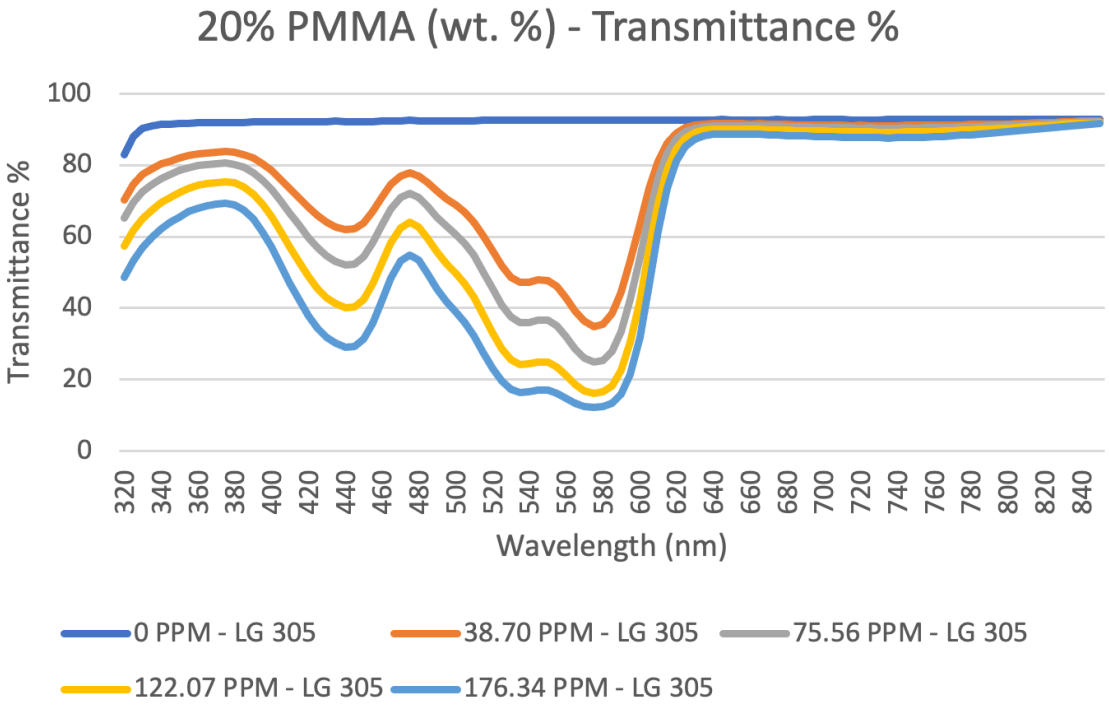

FIGURE 8.3: Transmission results of 20% PMMA infused with Lumogen f red 305 measured on Perkin Elmer Lambda 950 Spectrophotometer

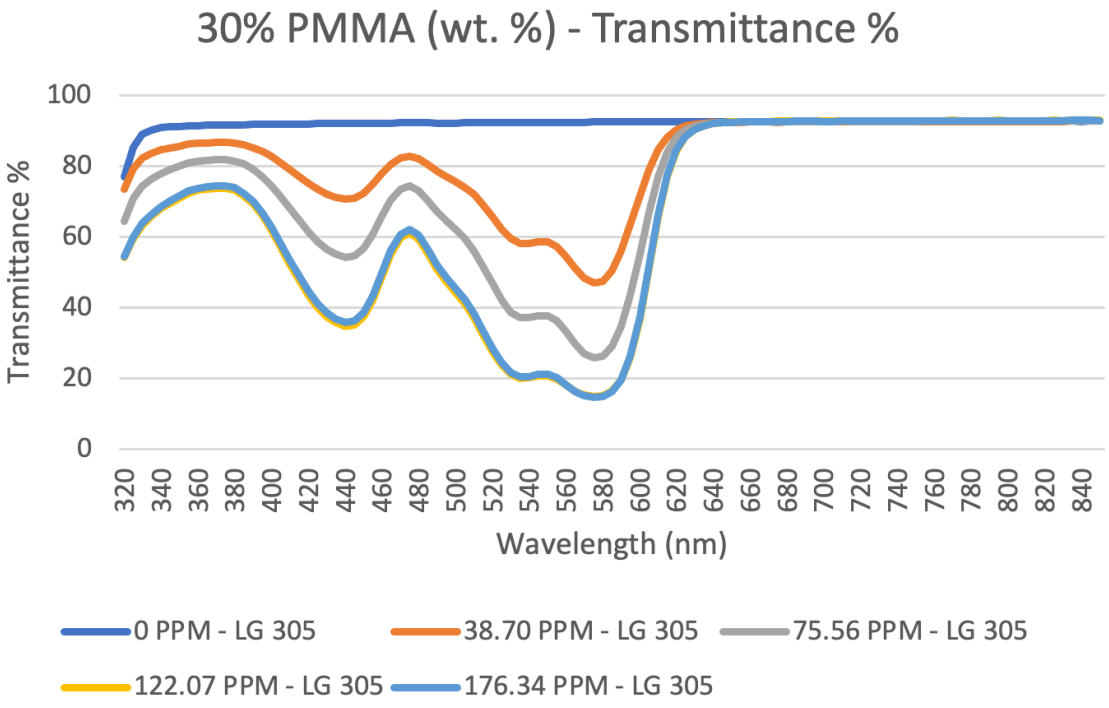

FIGURE 8.4: Transmission results of 30% PMMA infused with Lumogen f red 305 measured on Perkin Elmer Lambda 950 Spectrophotometer

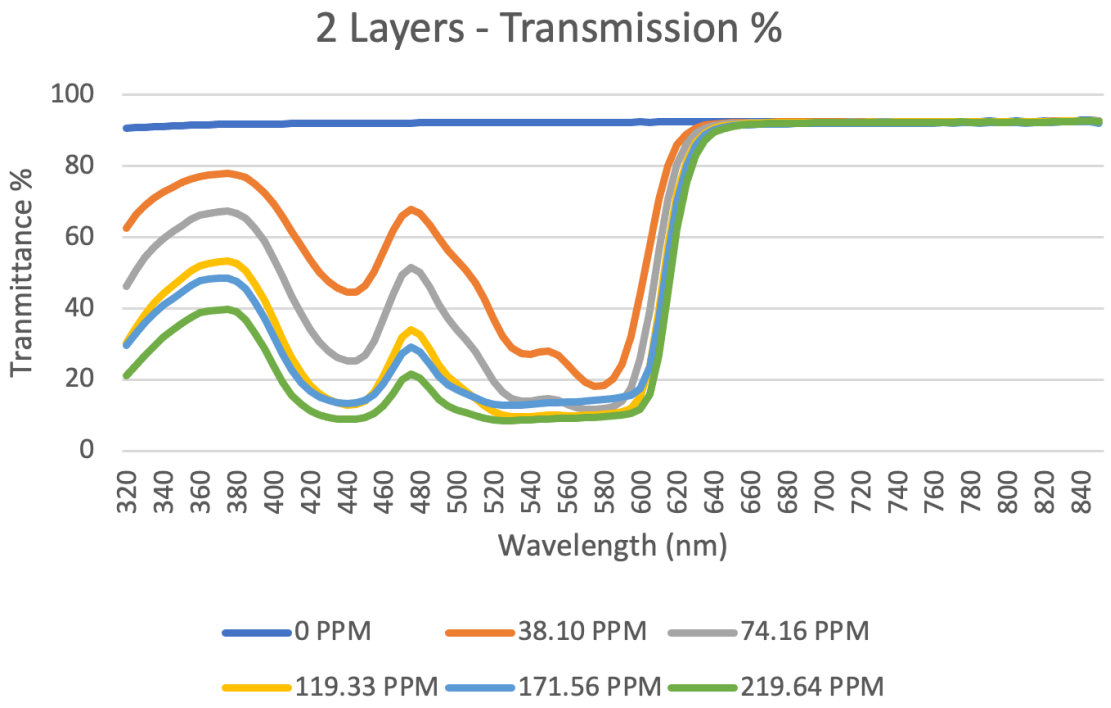

FIGURE 8.5: Transmission results of 2 layers of polymer layer infused with Lumogen f red 305 measured on Perkin Elmer Lambda 950 Spectrophotometer

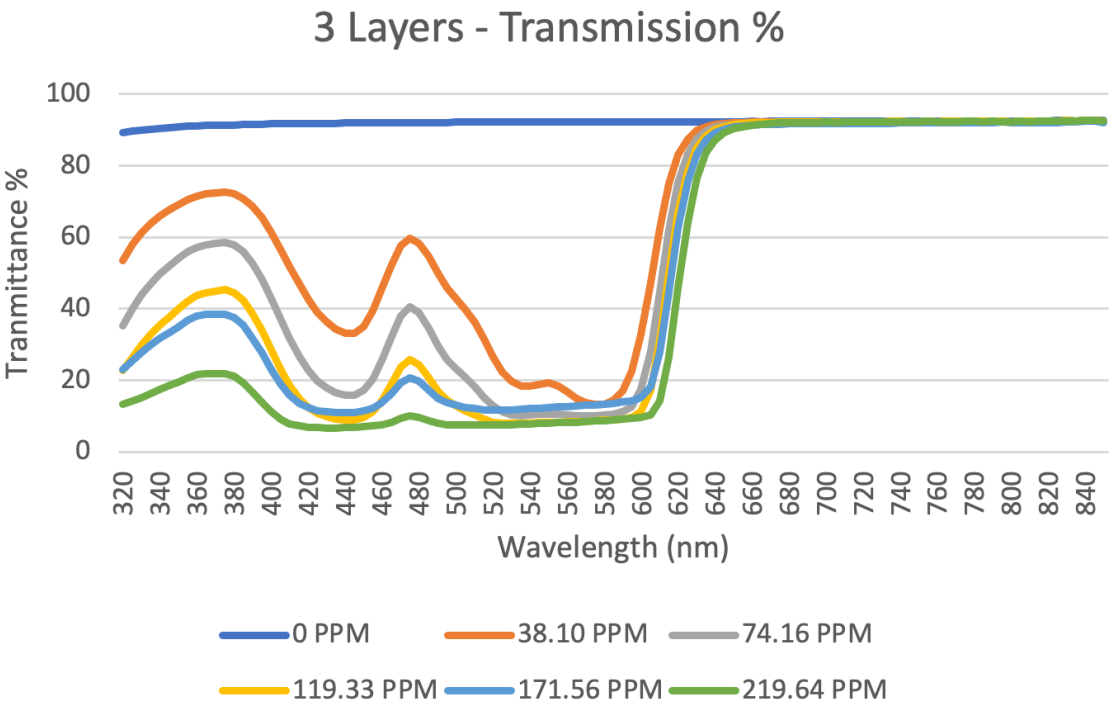

FIGURE 8.6: Transmission results of 3 layers of polymer layer infused with Lumogen f red 305 measured on Perkin Elmer Lambda 950 Spectrophotometer

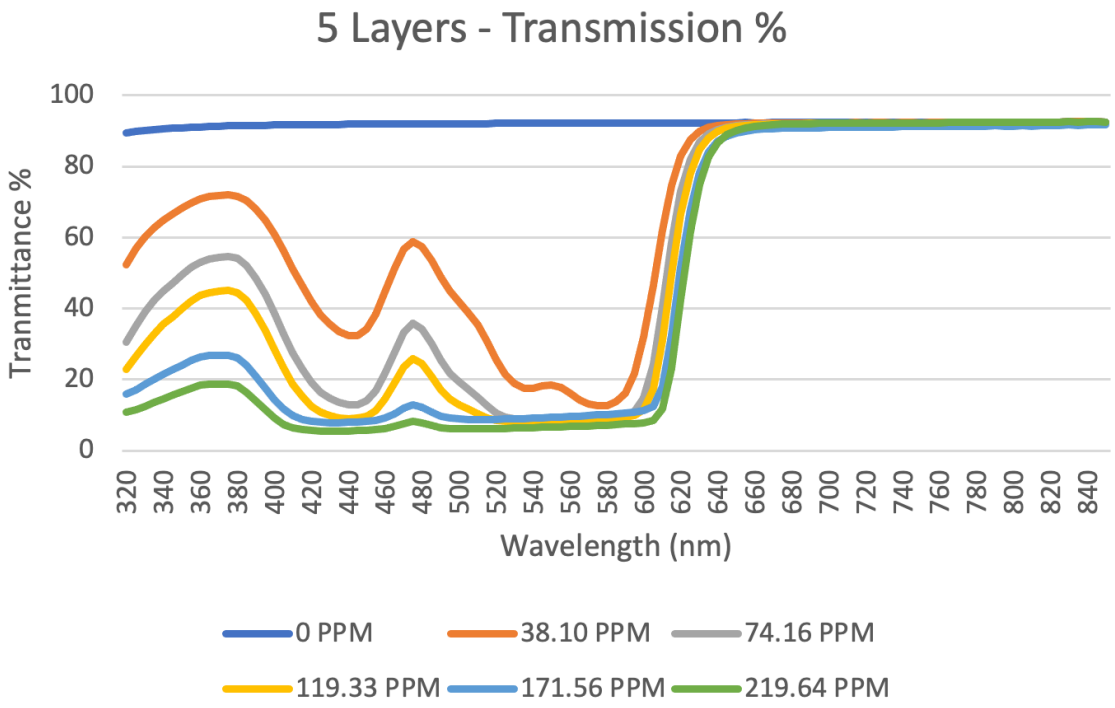

FIGURE 8.7: Transmission results of 5 layers of polymer layer infused with Lumogen f red 305 measured on Perkin Elmer Lambda 950 Spectrophotometer

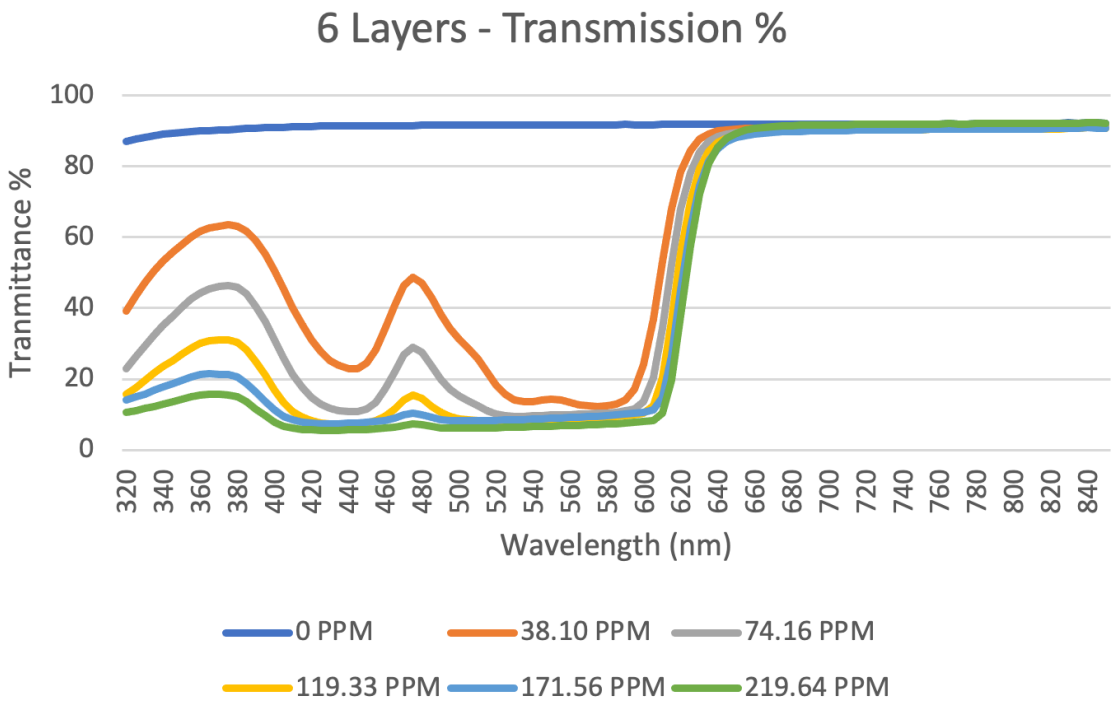

FIGURE 8.8: Transmission results of 6 layers of polymer layer infused with Lumogen f red 305 measured on Perkin Elmer Lambda 950 Spectrophotometer

8.2.2 Reflection graphs

This section contains all the reflectance graphs for the measured samples.

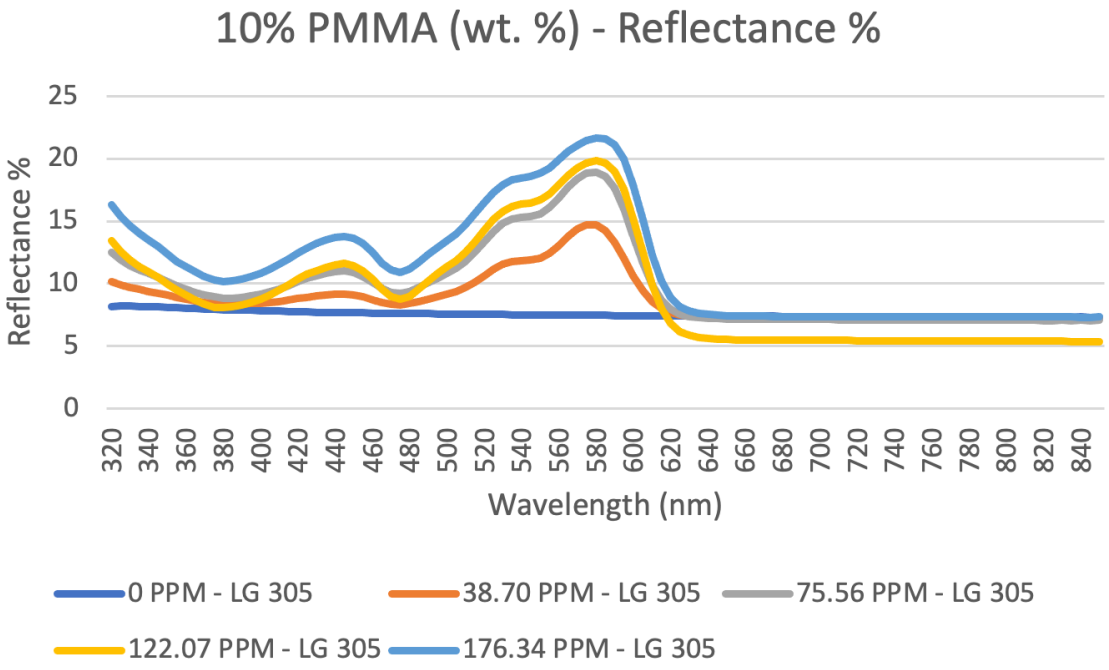

FIGURE 8.9: Reflectance results of 10% PMMA infused with Lumogen f red 305 measured on Perkin Elmer Lambda 950 Spectrophotometer

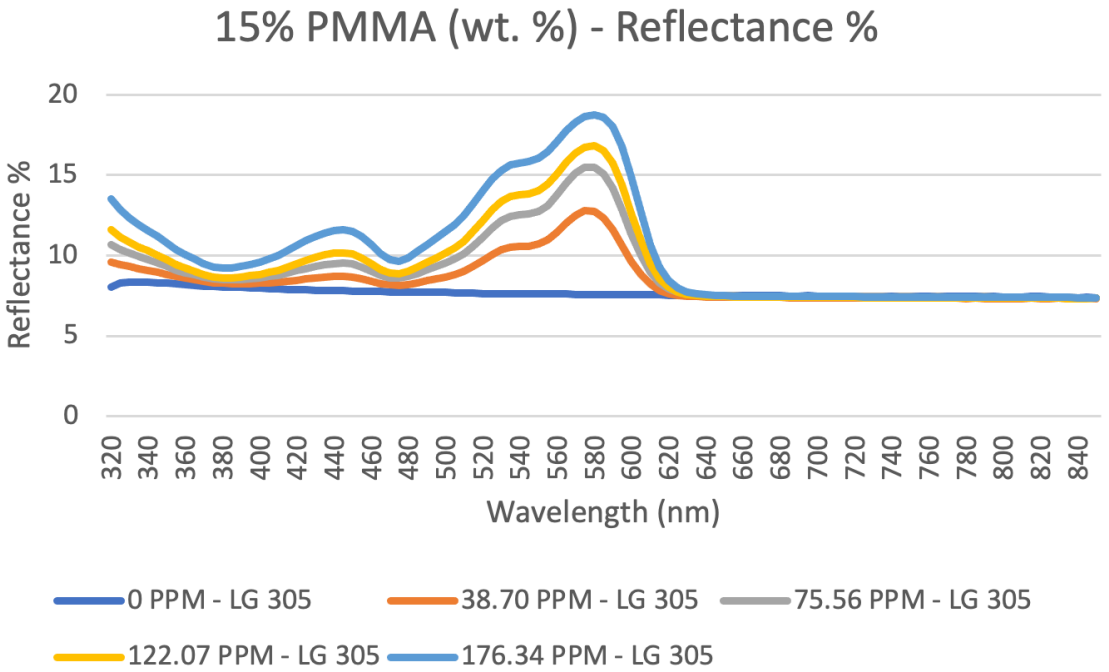

FIGURE 8.10: Reflectance results of 15% PMMA infused with Lumogen f red 305 measured on Perkin Elmer Lambda 950 Spectrophotometer

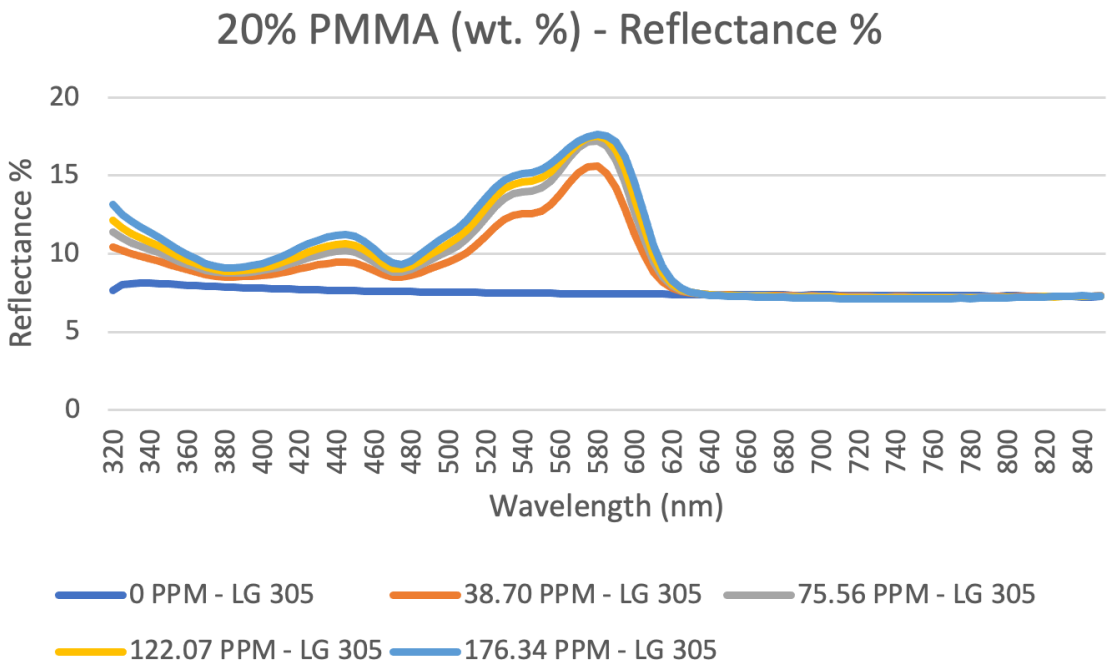

FIGURE 8.11: Reflectance results of 20% PMMA infused with Lumogen f red 305 measured on Perkin Elmer Lambda 950 Spectrophotometer

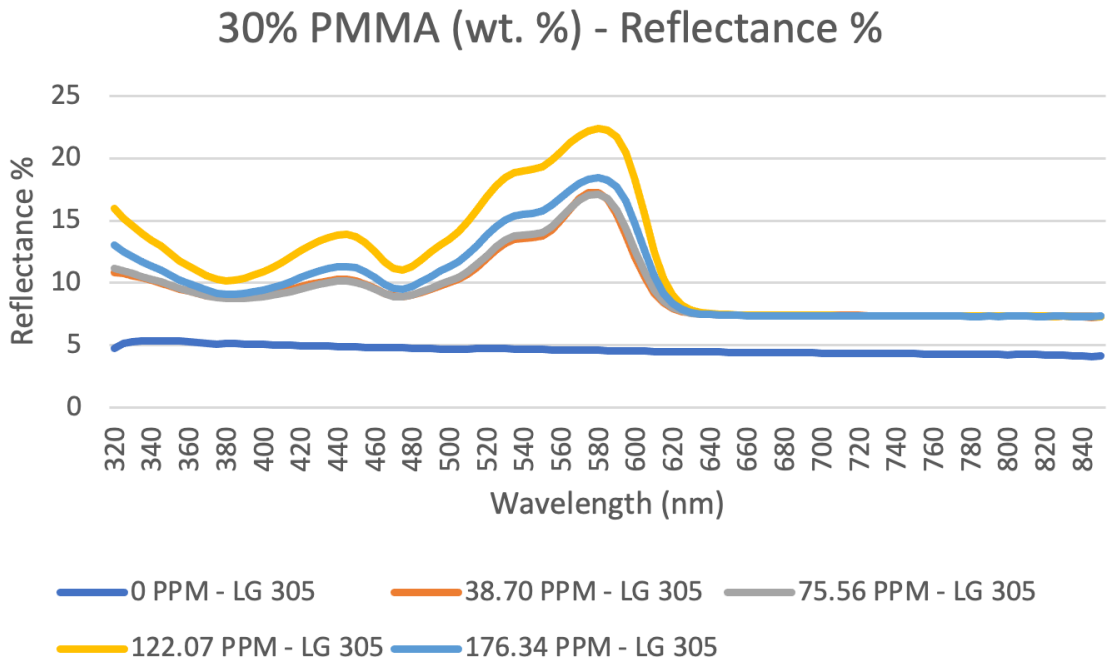

FIGURE 8.12: Reflectance results of 30% PMMA infused with Lumogen f red 305 measured on Perkin Elmer Lambda 950 Spectrophotometer

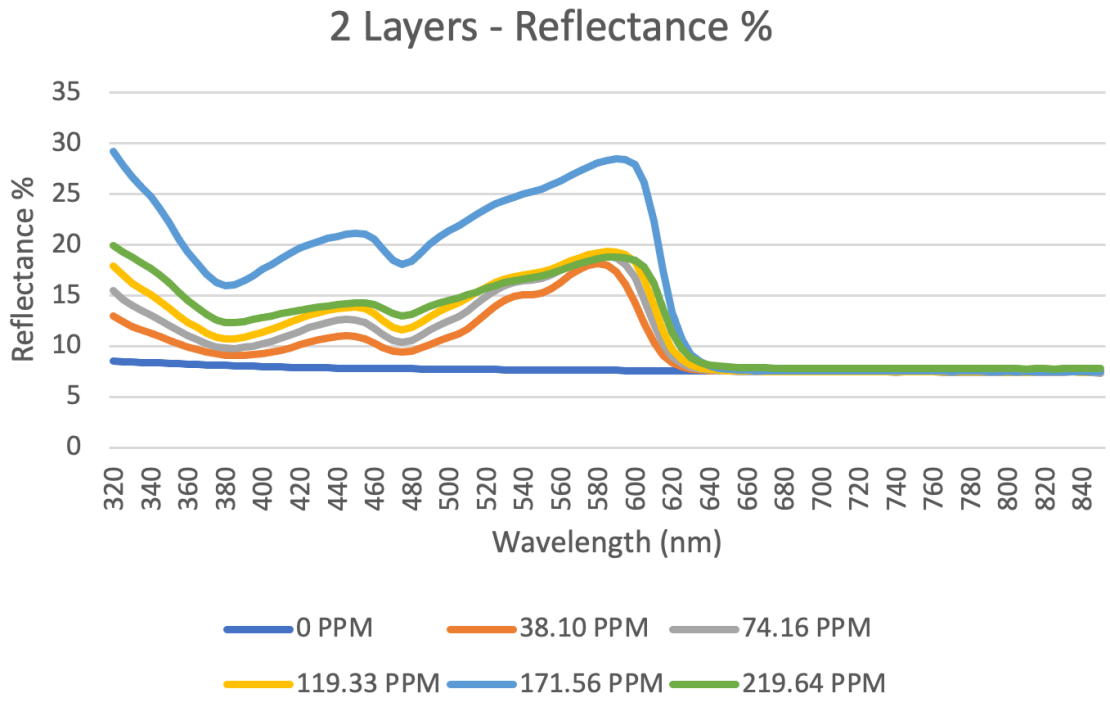

FIGURE 8.13: Reflectance results of 2 layers of polymer layer infused with Lumogen f red 305 measured on Perkin Elmer Lambda 950 Spectrophotometer

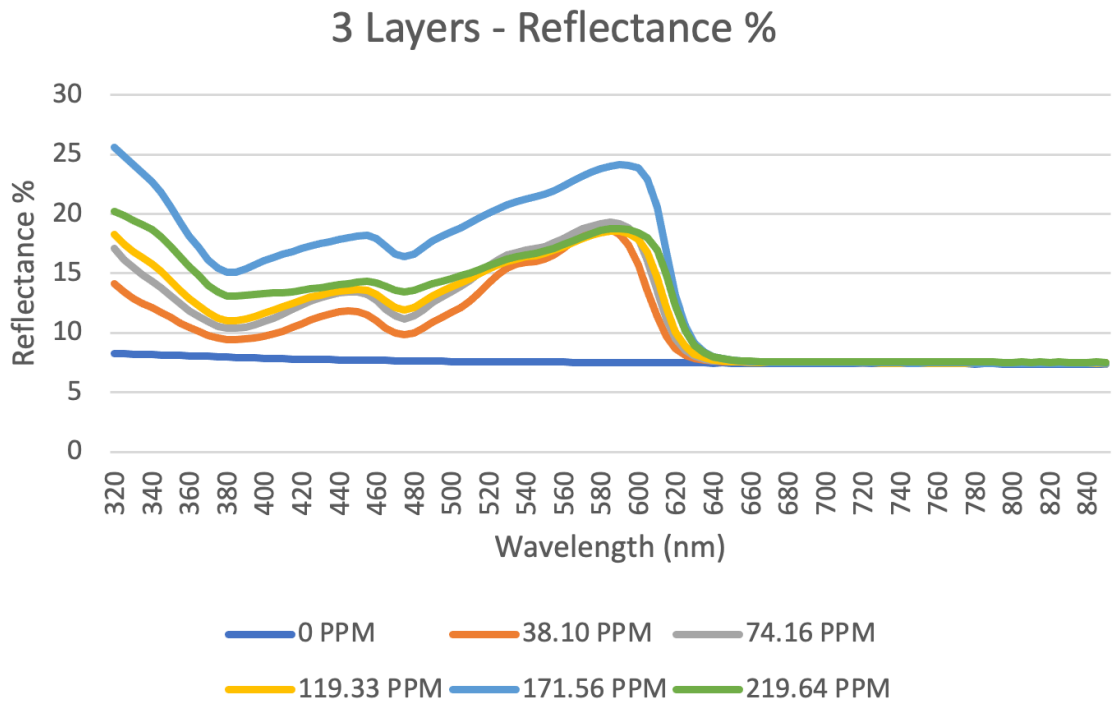

FIGURE 8.14: Reflectance results of 3 layers of polymer layer infused with Lumogen f red 305 measured on Perkin Elmer Lambda 950 Spectrophotometer

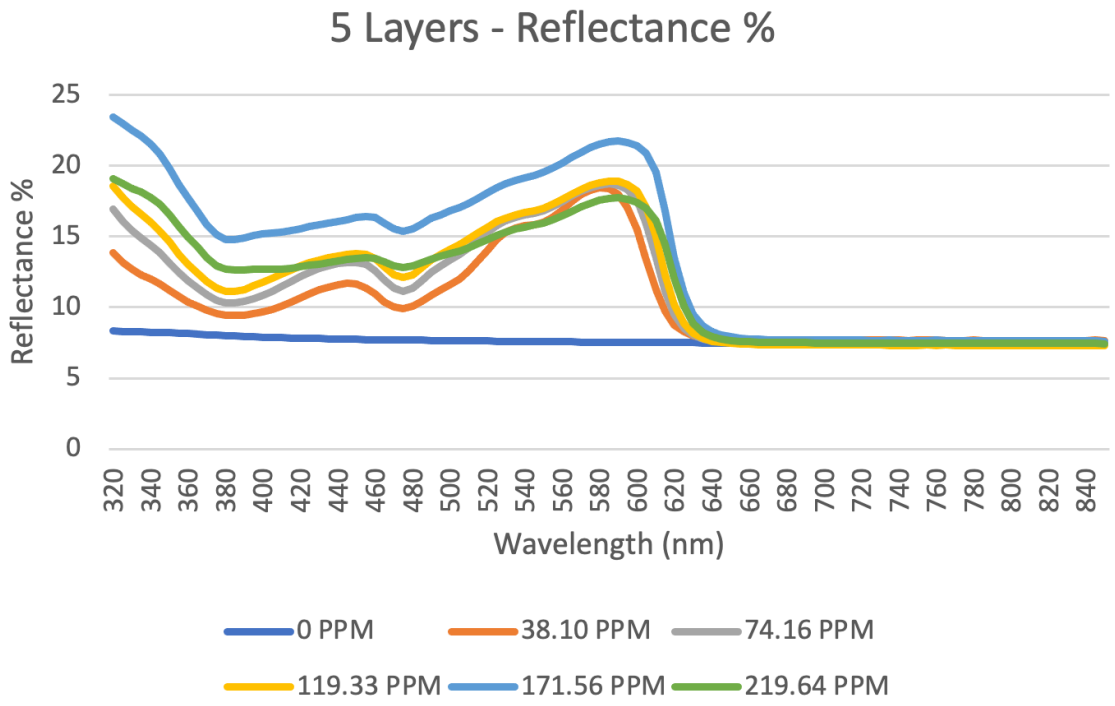

FIGURE 8.15: Reflectance results of 5 layers of polymer layer infused with Lumogen f red 305 measured on Perkin Elmer Lambda 950 Spectrophotometer

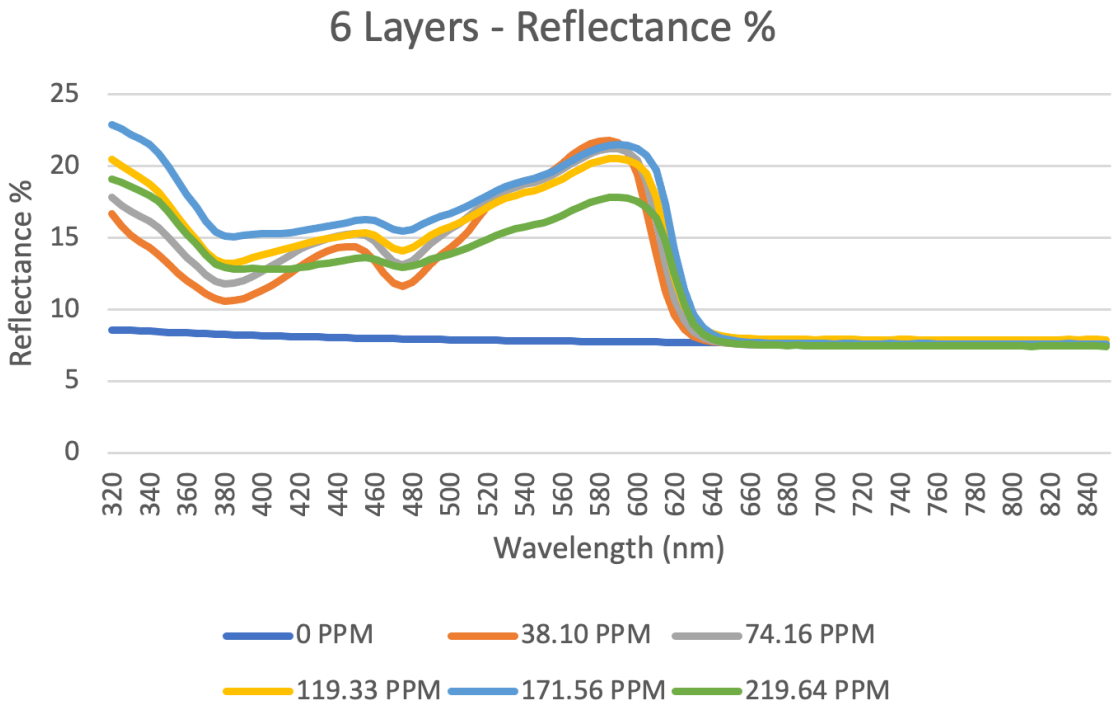

FIGURE 8.16: Reflectance results of 6 layers of polymer layer infused with Lumogen f red 305 measured on Perkin Elmer Lambda 950 Spectrophotometer

8.2.3 Absorption graphs

This section contains all the absorption graphs for the measured samples.

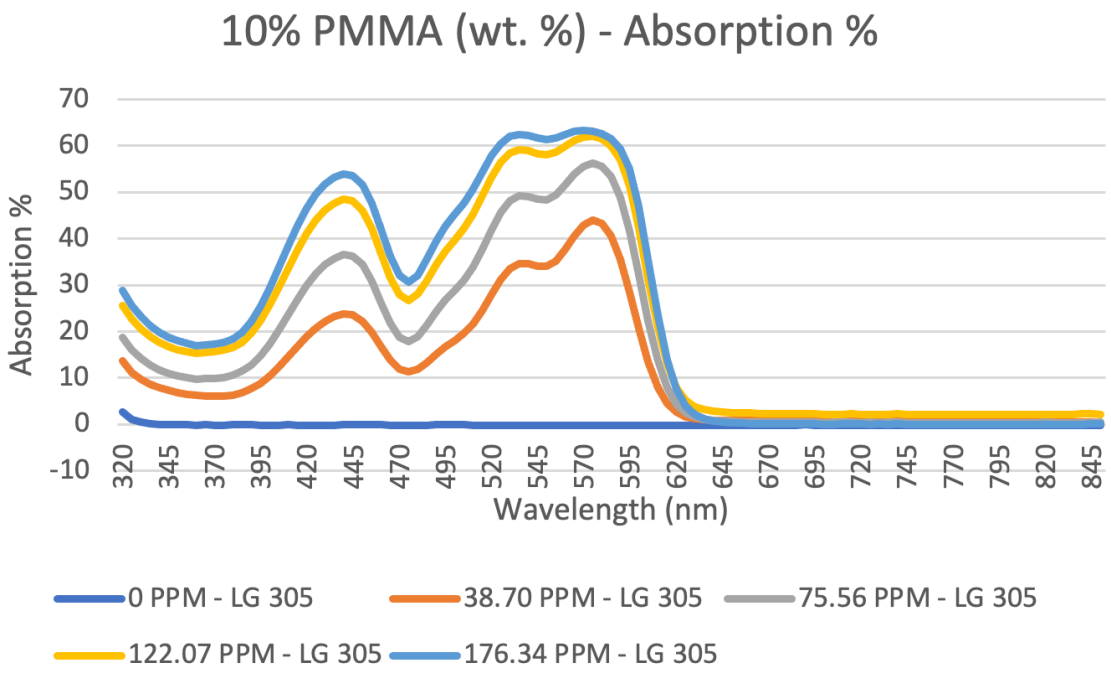

FIGURE 8.17: Absorption results of 10% PMMA infused with Lumogen f red 305 measured on Perkin Elmer Lambda 950 Spectrophotometer

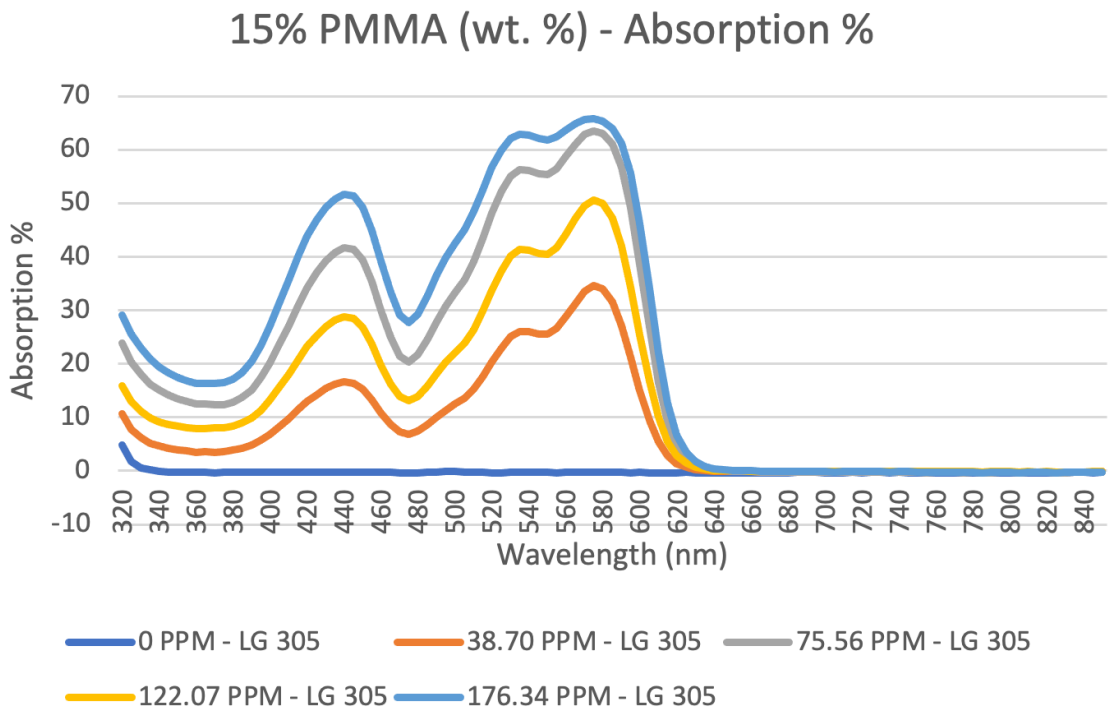

FIGURE 8.18: Absorption results of 15% PMMA infused with Lumogen f red 305 measured on Perkin Elmer Lambda 950 Spectrophotometer

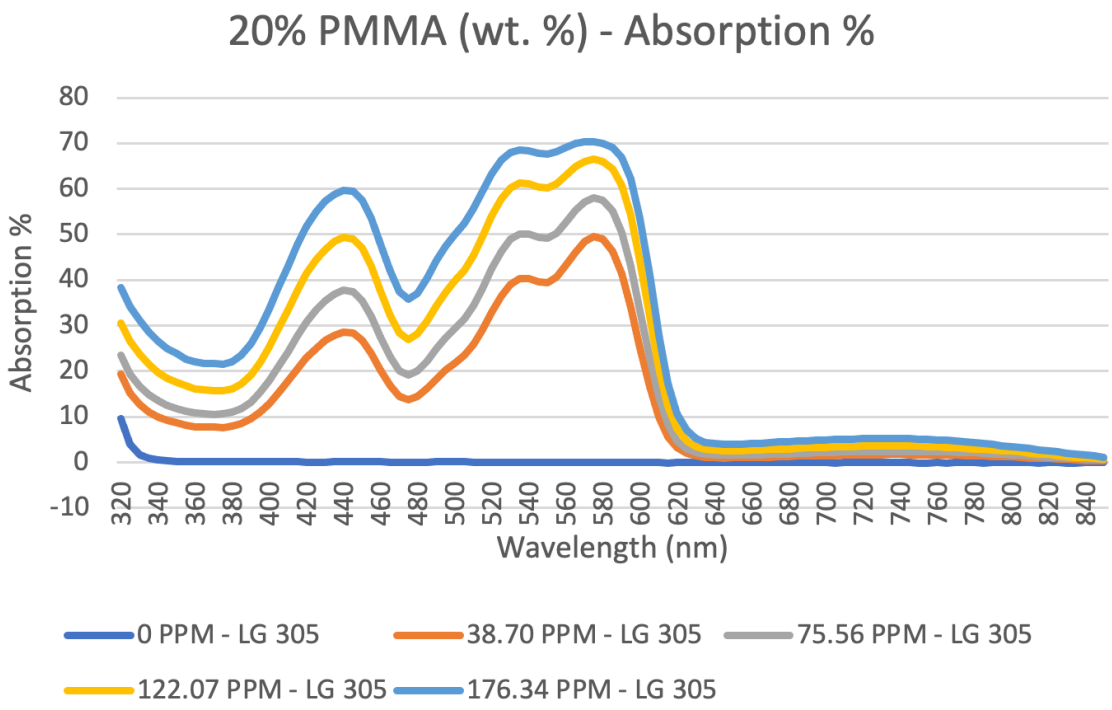

FIGURE 8.19: Absorption results of 20% PMMA infused with Lumogen f red 305 measured on Perkin Elmer Lambda 950 Spectrophotometer

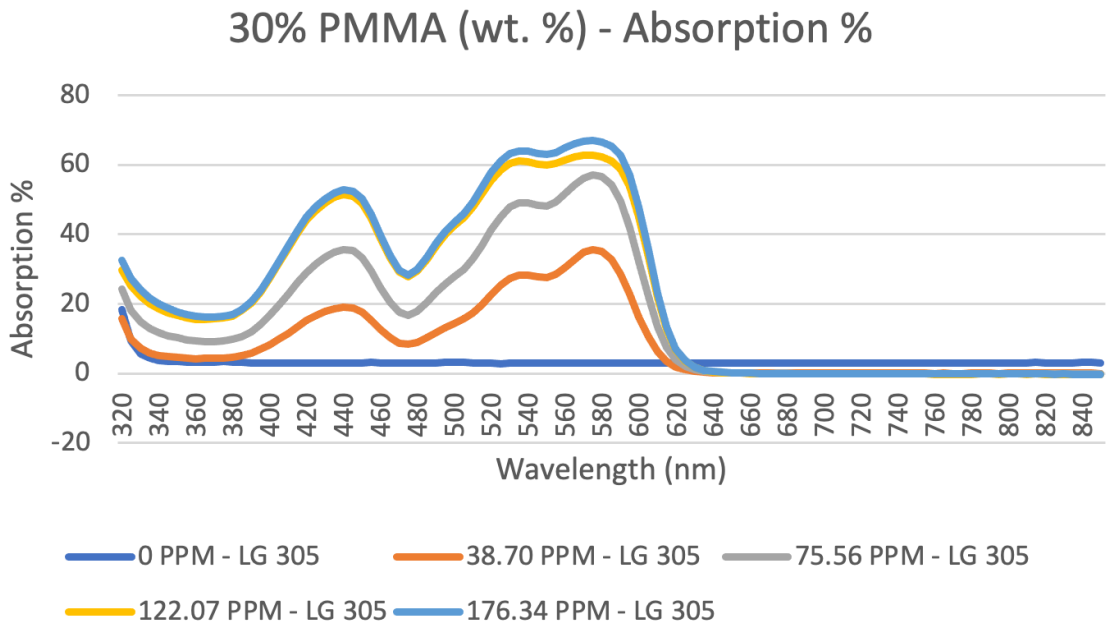

FIGURE 8.20: Absorption results of 30% PMMA infused with Lumogen f red 305 measured on Perkin Elmer Lambda 950 Spectrophotometer

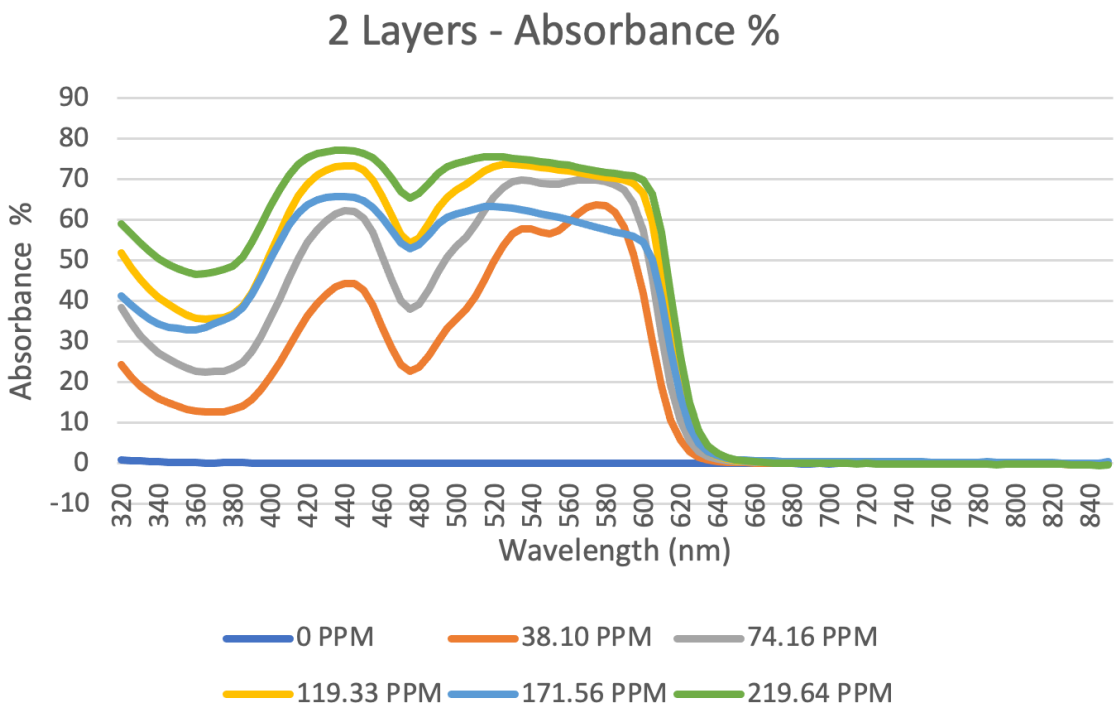

FIGURE 8.21: Absorption results of 2 layers of polymer layer infused with Lumogen f red 305 measured on Perkin Elmer Lambda 950 Spectrophotometer

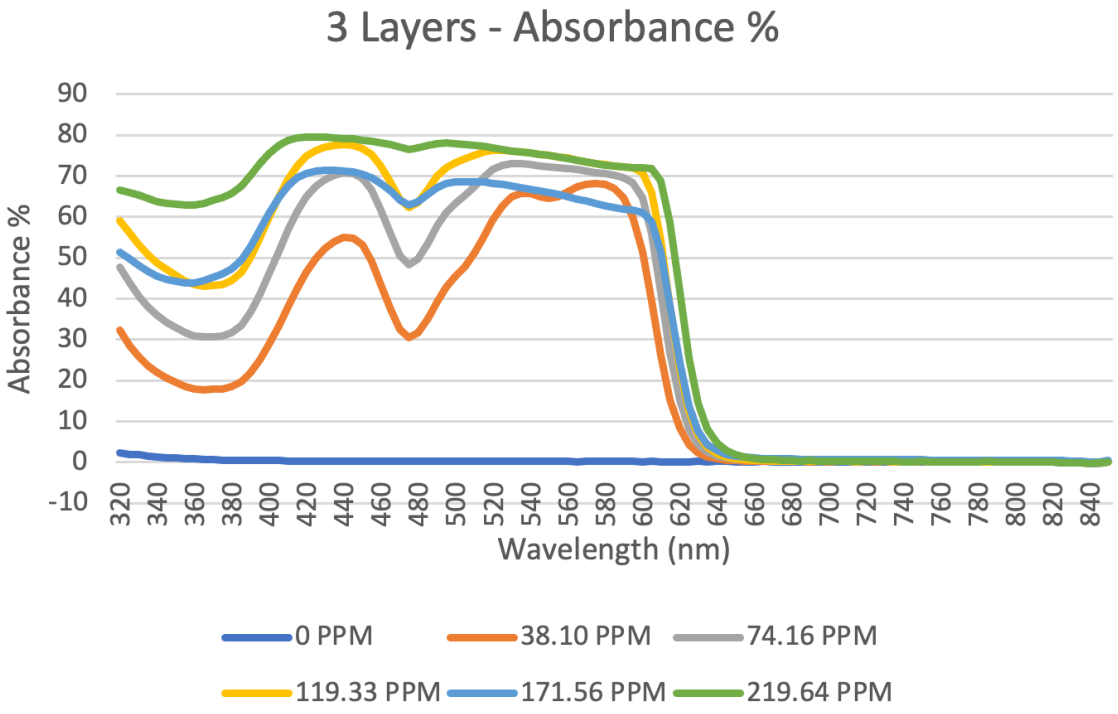

FIGURE 8.22: Absorption results of 3 layers of polymer layer infused with Lumogen f red 305 measured on Perkin Elmer Lambda 950 Spectrophotometer

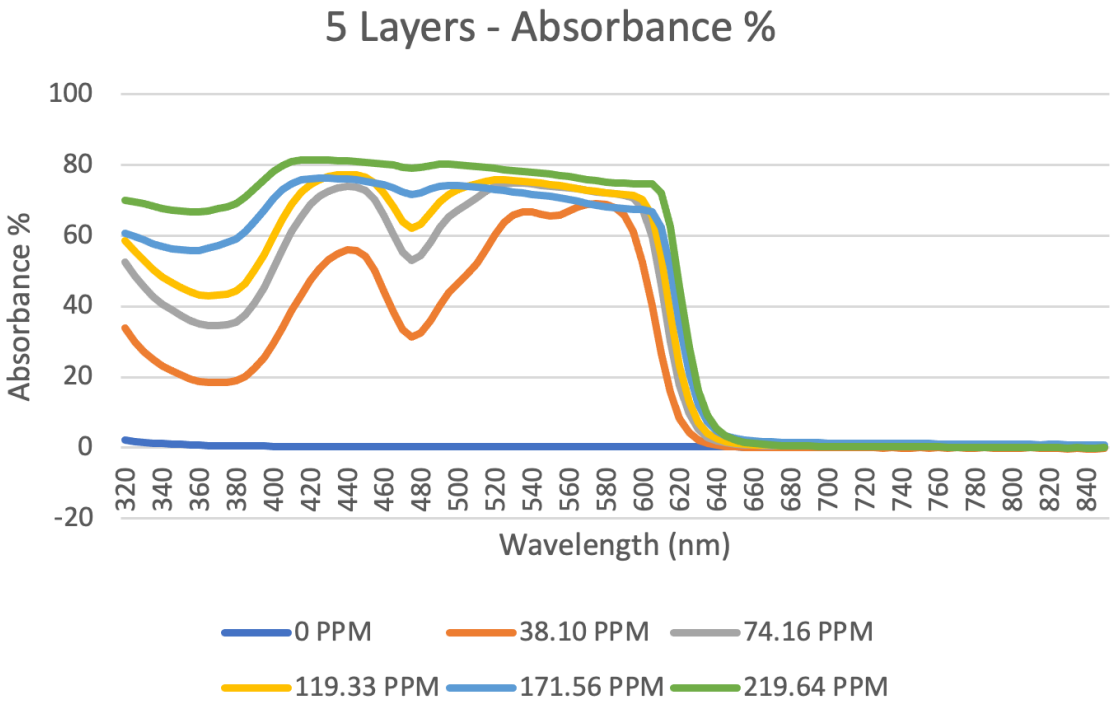

FIGURE 8.23: Absorption results of 5 layers of polymer layer infused with Lumogen f red 305 measured on Perkin Elmer Lambda 950 Spectrophotometer

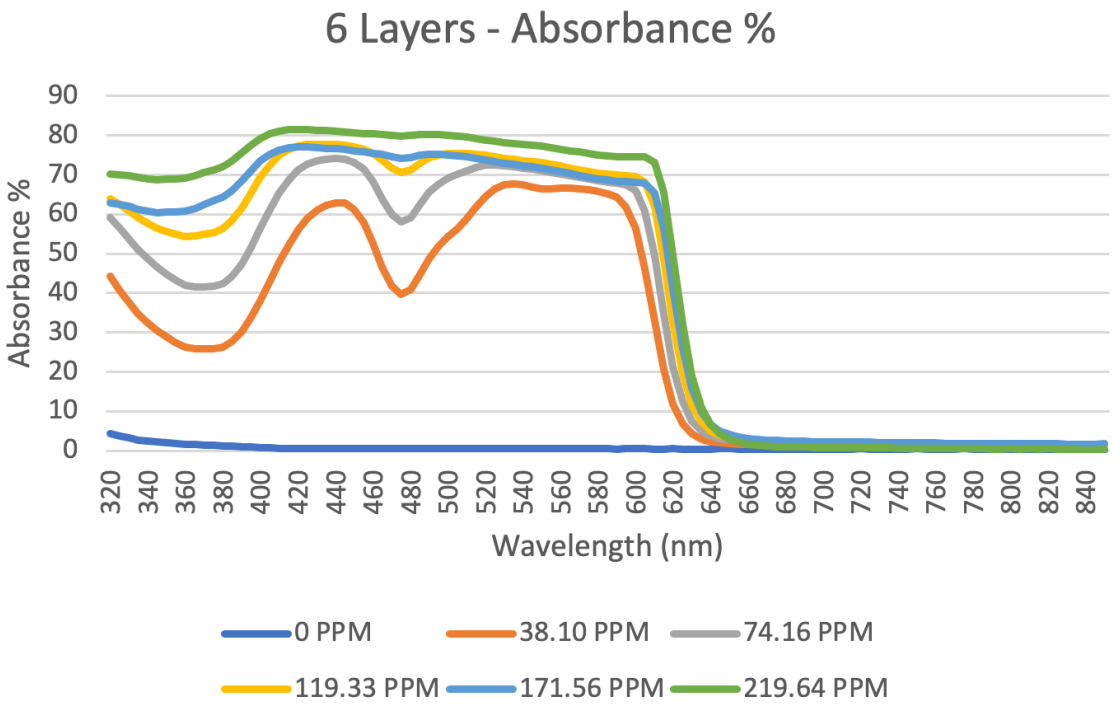

FIGURE 8.24: Absorption results of 6 layers of polymer layer infused with Lumogen f red 305 measured on Perkin Elmer Lambda 950 Spectrophotometer

8.3 Appendix III

8.3.1 Graphs from Laser Measurements

This section gives the graphs that are taken for the green laser measurement for photoluminescent external quantum efficiency for 6 layer 38.10 PPM concentration.

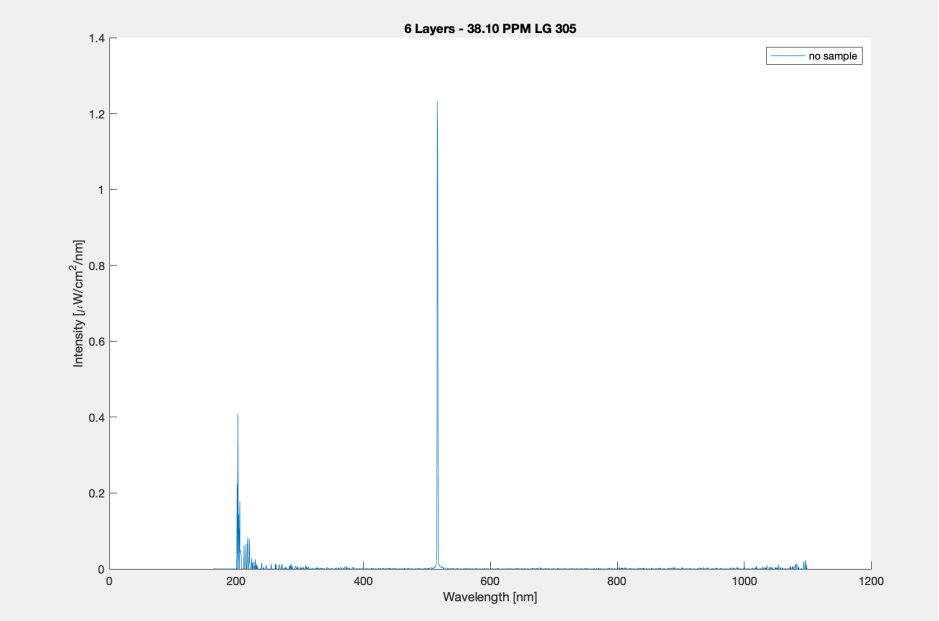

FIGURE 8.25: Figure depicts the measurements that are performed without a sample with green laser

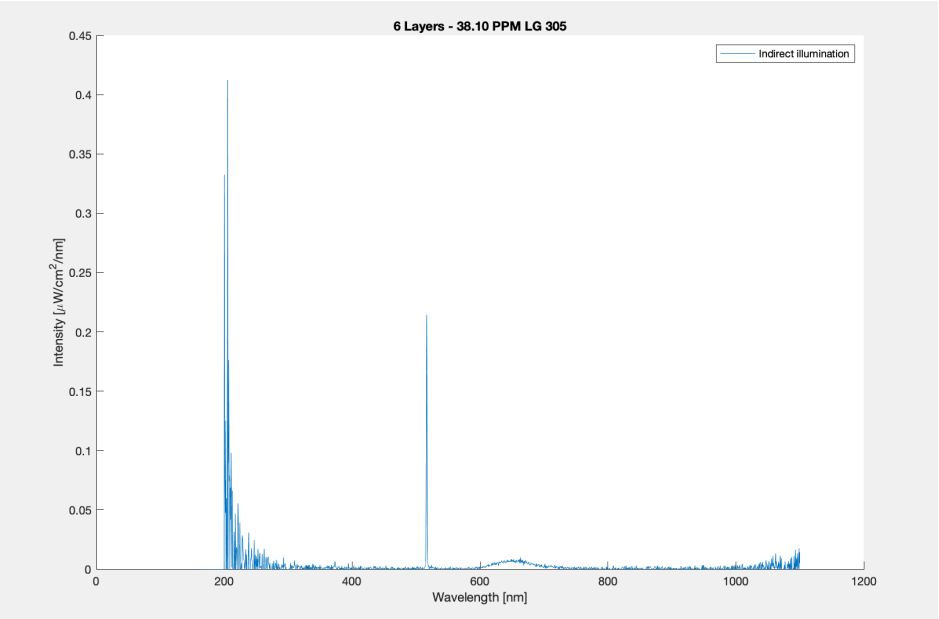

FIGURE 8.26: Figure depicts the measurements that are performed with sample hitting the walls of the integrating sphere with green laser

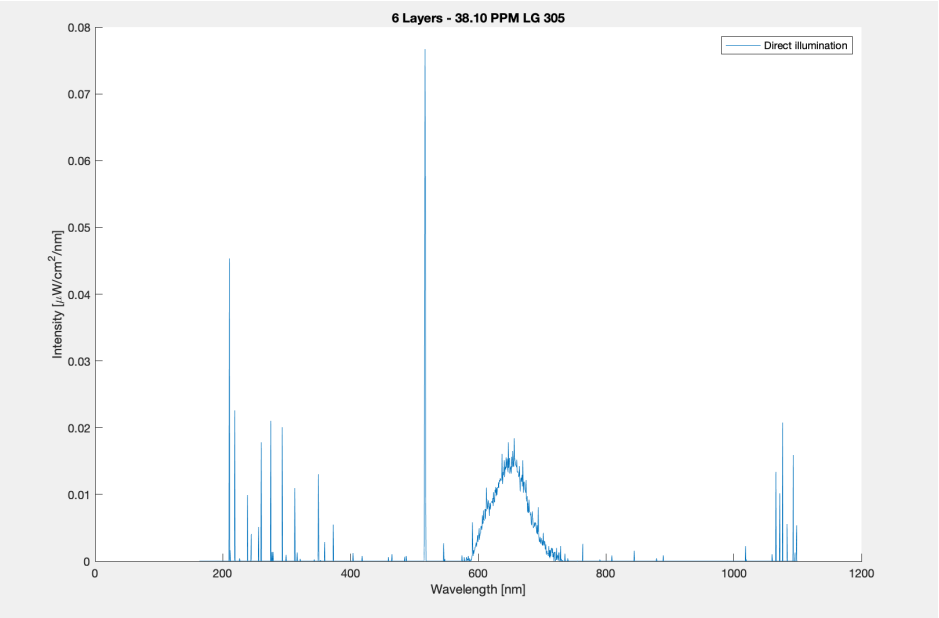

FIGURE 8.27: Figure depicts the measurements that are performed with sample hitting the sample directly with green laser

8.3.2 Photoluminiscent Efficiency by intensity of light

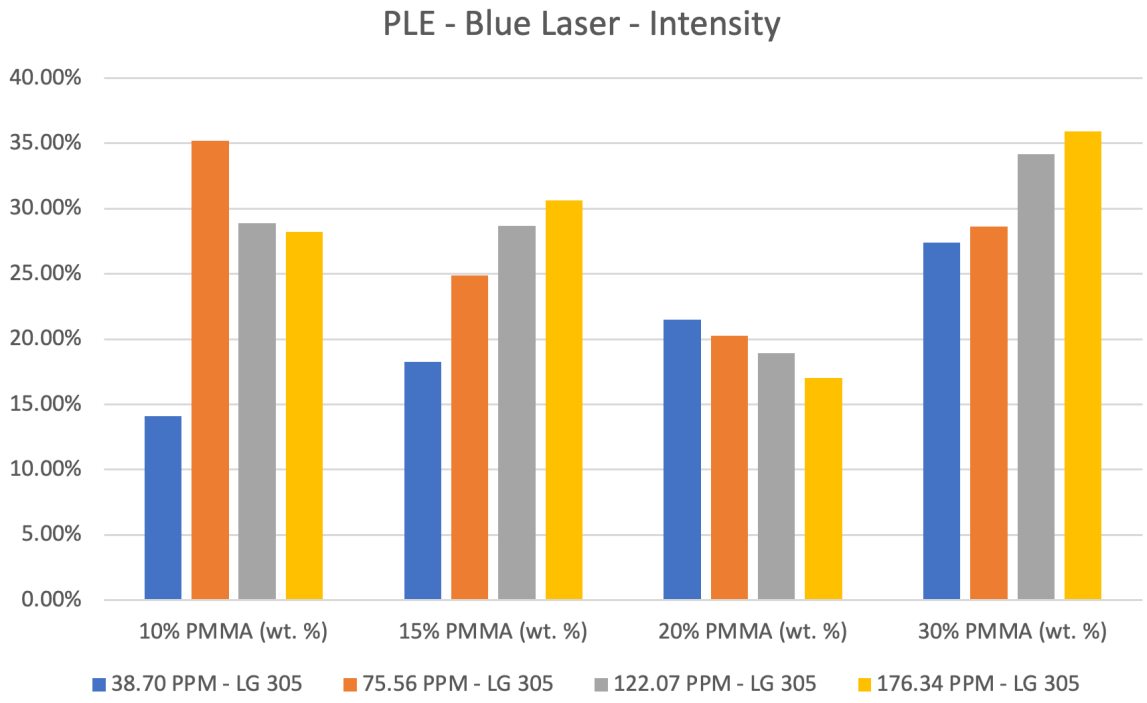

FIGURE 8.28: Figure depicts the photoluminescent external efficiency of solid polymer layer with blue laser excitation

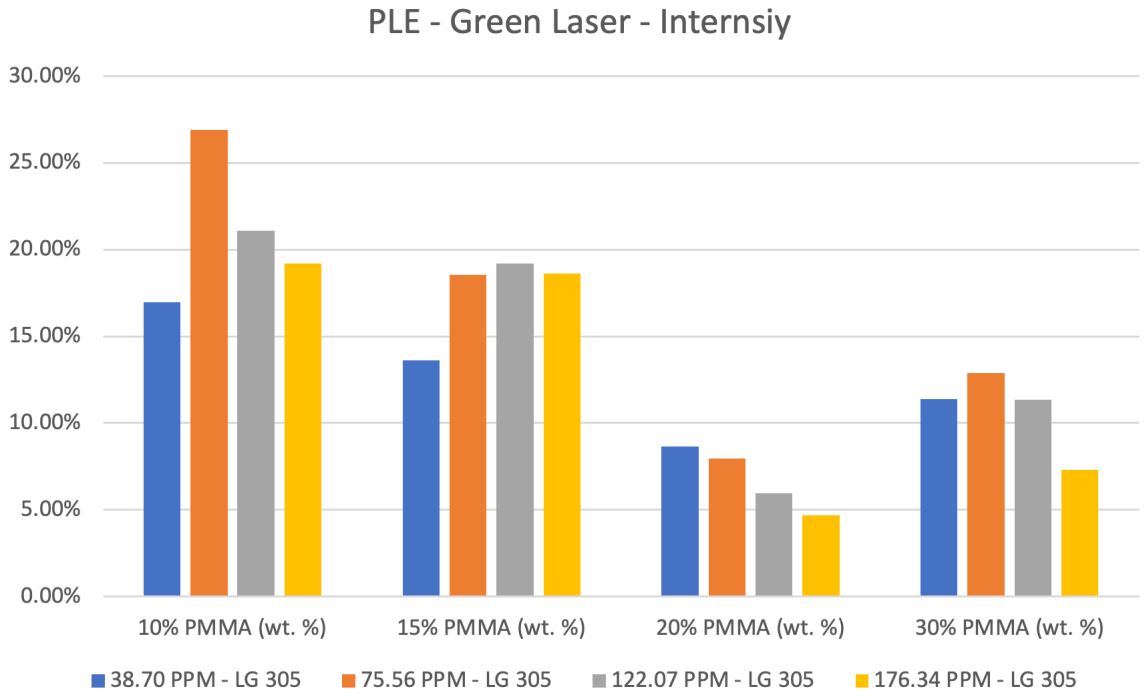

FIGURE 8.29: Figure depicts the photoluminescent external efficiency of solid polymer layer with green laser excitation

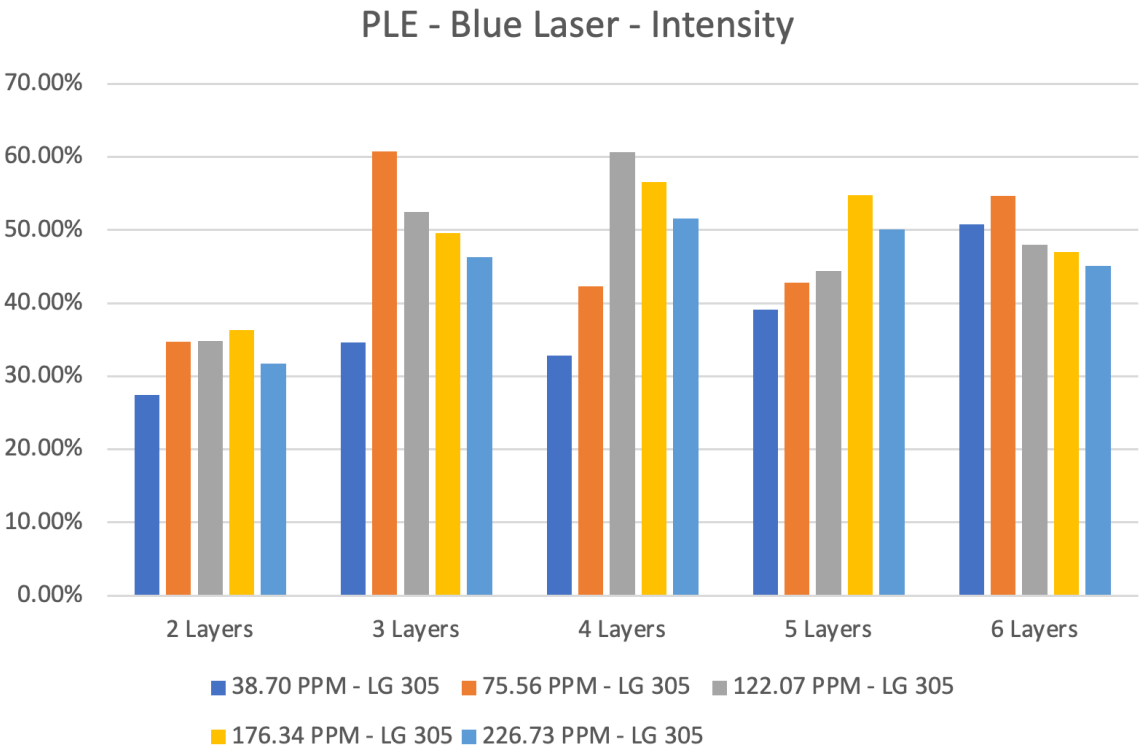

FIGURE 8.30: Figure depicts the photoluminescent external efficiency of solid polymer layer with blue laser excitation

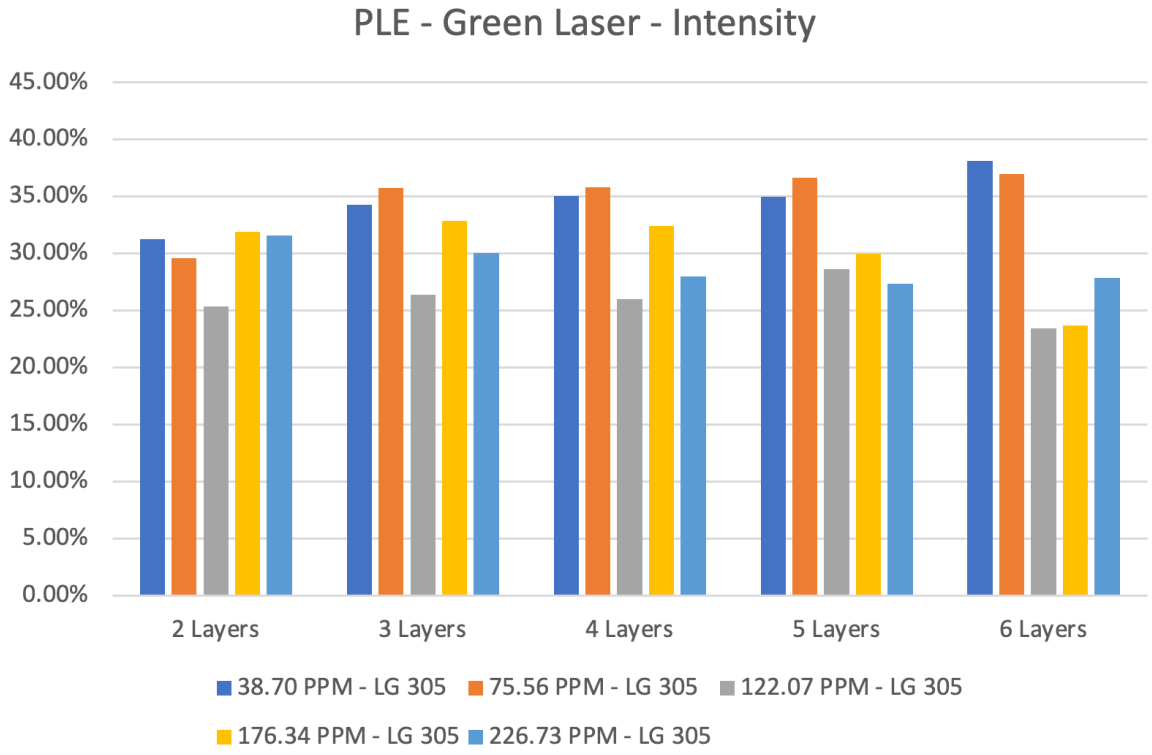

FIGURE 8.31: Figure depicts the photoluminescent external efficiency of solid polymer layer with green laser excitation

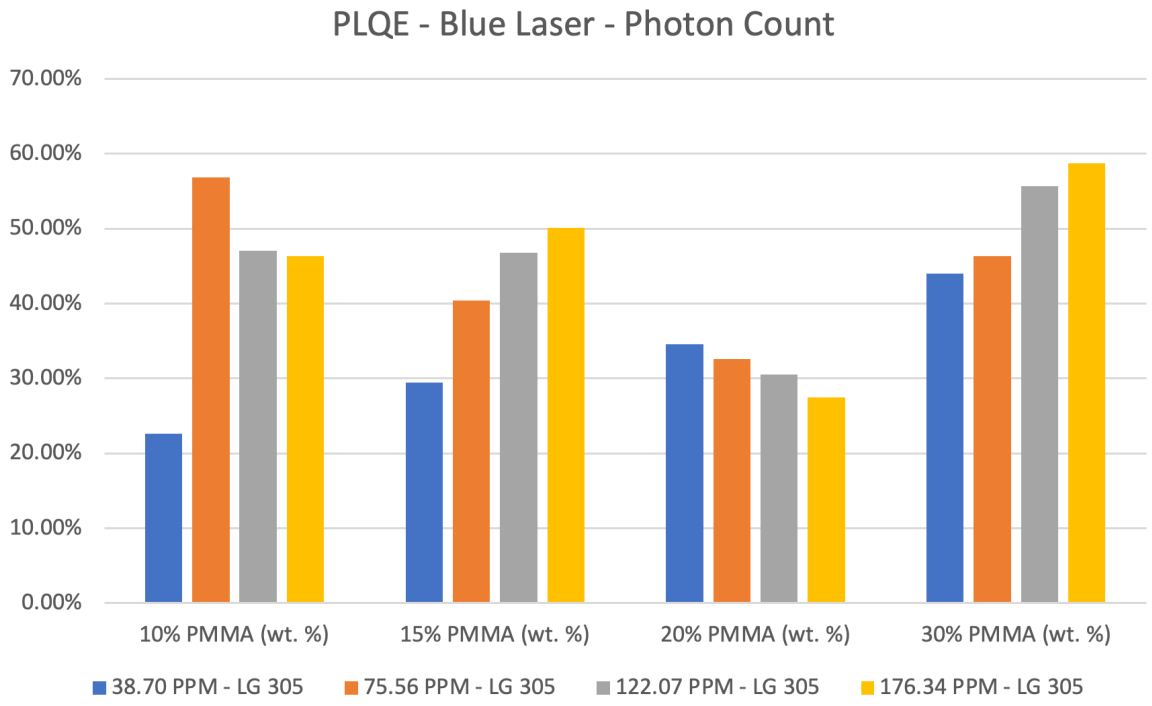

FIGURE 8.32: Figure depicts the photoluminescent external quantum efficiency of solid polymer layer with blue laser excitation

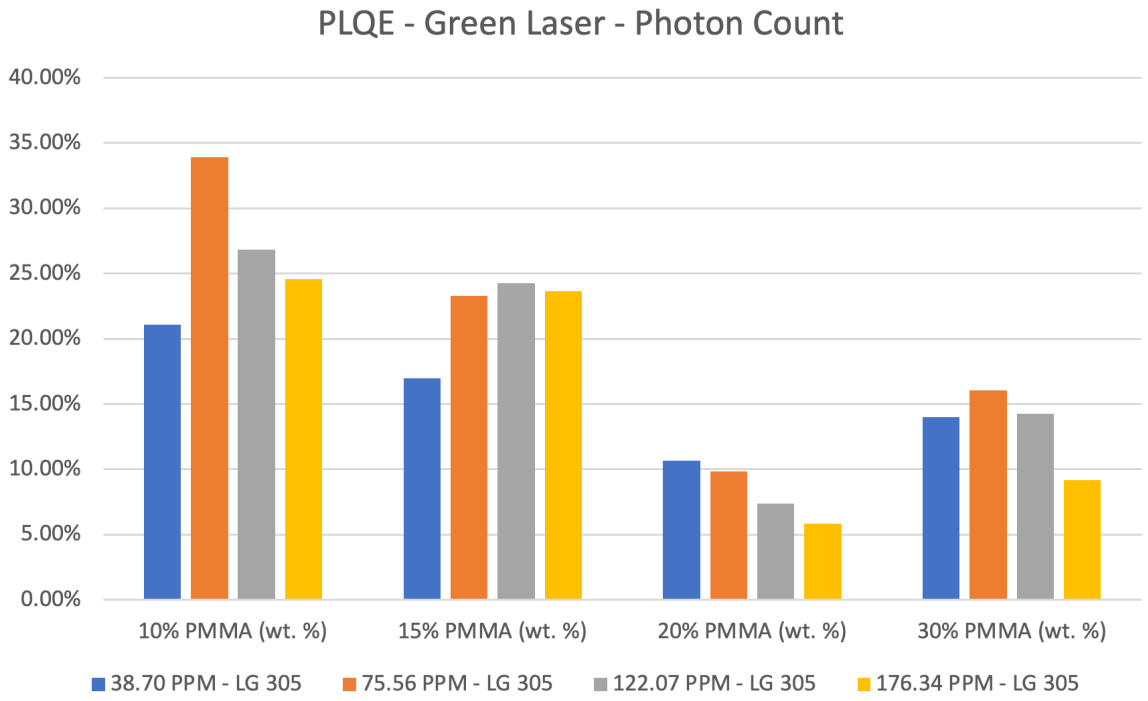

FIGURE 8.33: Figure depicts the photoluminescent external quantum efficiency of solid polymer layer with green laser excitation

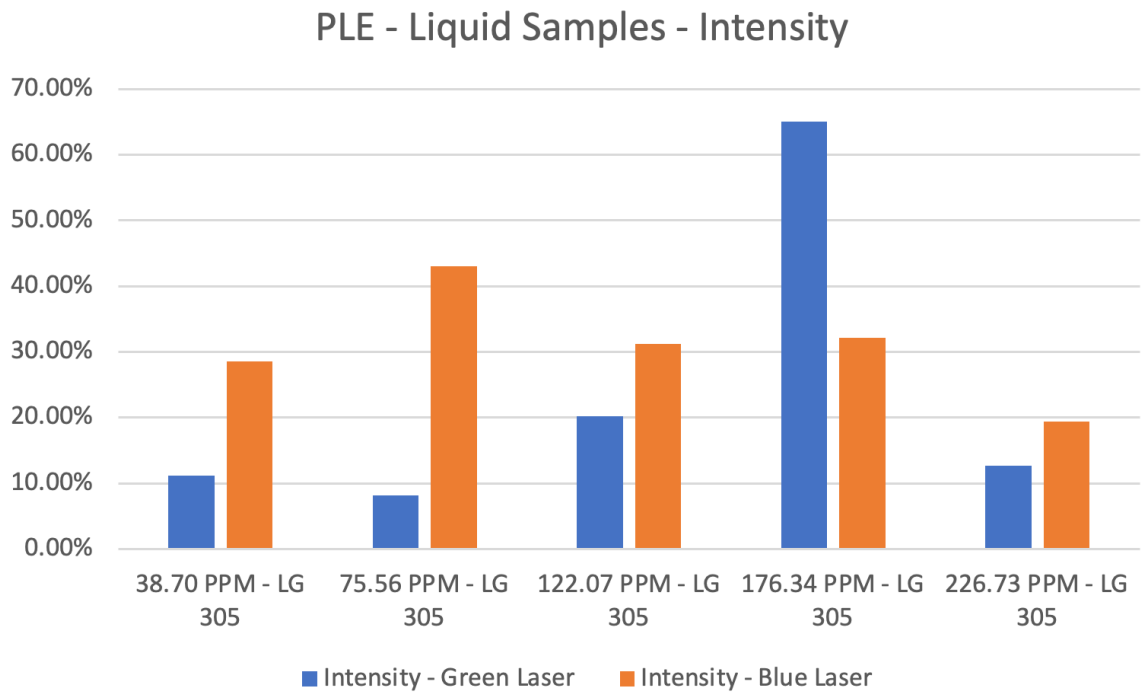

FIGURE 8.34: Figure depicts the photoluminescent external efficiency of Liquid polymer layer with blue, green laser excitation